**Noname manuscript No.**
(will be inserted by the editor)

# Chattering: An overlooked peculiarity of rocking motion

**Anastasios I. Giouvanidis*** · **Elias G. Dimitrakopoulos** · **Paulo B. Lourenço**

Received: date / Accepted: date

**Abstract** *Complete chattering* occurs when a structure undergoes a theoretically infinite sequence of impacts in finite time, that eventually bring the structure to the state of persistent (continuous) contact. This study investigates the conditions under which a rigid rocking block undergoes complete chattering when subjected to sinusoidal ground excitation. The analysis explains how the acceleration amplitude of the ground excitation affects the chattering time. It also proves that there exists a (sinusoidal) ground acceleration amplitude, below which rocking motion terminates even under a nonzero ground excitation, almost independently of the frequency of the ground excitation. Furthermore, the study adopts perturbation theory and proposes an asymptotic approximation of the time needed for chattering to be completed, i.e. *chattering time*. It then verifies the asymptotic approximation using an independent semi-analytical approach. Overall, the results highlight the importance of complete chattering on the dynamic rocking response; a feature of nonlinear dynamics which is often overlooked in earthquake engineering.

Anastasios I. Giouvanidis, *Corresponding Author
Department of Civil Engineering, ISISE, University of Minho, 4800-058 Guimarães, Portugal
E-mail: agiouvanidis@civil.uminho.pt

Elias G. Dimitrakopoulos
Department of Civil and Environmental Engineering, The Hong Kong University of Science and Technology, Clear Water Bay, Hong Kong, China
E-mail: ilias@ust.hk

Paulo B. Lourenço
Department of Civil Engineering, ISISE, University of Minho, 4800-058 Guimarães, Portugal
E-mail: pbl@civil.uminho.pt

**Keywords** rocking · chattering · perturbation theory · asymptotic analysis · impact

## 1 Introduction

Rocking motion is increasingly being investigated as a means to isolate structures from ground excitations by allowing rigid body rotation. Subsequently, it finds application on a variety of engineering projects, e.g. from freestanding contents [22, 39, 40] and classical monuments [23, 49, 63] to modern buildings and bridges [2, 18, 21, 26, 28, 54, 59–61]. From an earthquake engineering perspective, the transient response of a rocking structure under a finite duration ground excitation is of primary importance, as it directly relates to seismic safety and structural failure [15, 19, 45, 55, 56, 62]. The dynamics of a (slender) freestanding rigid structure rocking on a rigid surface, without sliding or bouncing, when subjected to horizontal ground excitation is a classical problem which has been investigated in various scientific fields [35]. Despite the apparent structural simplicity, rocking motion is characterised by various nonlinear and nonsmooth dynamic phenomena, which compose a complex [64] and often chaotic behaviour [33, 37, 46].

*Chattering* is a feature of nonlinear dynamics that might appear during low amplitude oscillations, and is also evident in rocking motion. Chattering can be either *complete* or *incomplete* [8, 51]. Complete chattering refers to a sequence of theoretically infinite in number low velocity impacts that occur in finite time, and result in the structure coming to rest, even under nonzero ground excitation. Chattering is completed when a change in the state of contact, from instantaneous (i.e. impacts) to persistent (i.e. continuous con-

tact), takes place. At that time-instant, an *accumulation* (or *Zeno*) point appears in the response. Incomplete chattering refers to the case in which the sequence of low velocity impacts terminates without bringing the structure to rest. An intuitive illustration of complete chattering is a ball bouncing under gravity on an obstacle, exhibiting a theoretically infinite number of impacts till it comes to rest in finite time [14, 32, 43, 47, 53, 57]. Complete chattering is also observed in the motion of a falling rod [30, 31], the motion of the Euler's disk just before reaching its final singularity [42], and the inverted pendulum bouncing on lateral side-walls [8, 13, 44, 58].

Chattering is a highly nonlinear phenomenon that has been investigated in many fields of engineering (see e.g. Brogliato [6] and references therein). Two main research questions concern (i) the effect of chattering on the dynamic response, and (ii) the numerical challenges that emerge in simulations due to the presence of accumulation points.

With reference to the first question, Budd and Dux [8] showed that chattering is one of the main reasons of chaotic behaviour of impact oscillators. That study also revealed that small changes at the initial conditions can transform chattering from complete to incomplete. Baranyai and Várkonyi [5] investigated the initial conditions that engender complete chattering, and subsequently accumulation points, assuming frictionless impacts and ignoring any external force. A series of studies proposed Lyapunov-like conditions sufficient to restore stability to the structural system (i.e. Zeno stability) [29, 41]. Fewer studies focused on the time required till the accumulation point emerges, i.e. *chattering time*. Leine and Heimsch [43] and Or and Ames [52] adopted the Lyapunov stability theory [48] and proposed an upper bound of the finite chattering time for the bouncing ball problem. To address the same question, Demeio and Lenci [13] examined the inverted pendulum impacting on lateral side-walls and approximated the chattering time using asymptotic analysis.

The appearance of accumulation points creates numerical challenges/instabilities during simulation [52] as the persistent contact (corresponding to the accumulation point) is not described by the differential equation of motion [9, 43]. Such numerical challenges become even more complicated when impacts occur at multiple contact points. Different methods have been proposed to tackle such instability issues caused by the infinite number of impacts in finite time. One way is to bypass accumulation points (Nordmark and Piiroinen [51]) using an event-based algorithm, and thus, considering only finite, in number, impacts. Another approach is to approximate the accumulation points (Ames et al. [3]). It is also possible to suppress the spurious oscillations due to chattering (Acary [1]) via modifying the Moreau–Jean's time-stepping scheme [36, 50], increasing somewhat the energy dissipation. A popular approach is to adopt a velocity threshold to artificially terminate the motion of the structure once the velocity drops below that threshold (Chatterjee et al. [9] and Cosimo et al. [10]). A velocity threshold approach to tackle chattering in rocking simulations was also adopted in [18, 26, 27]. Alternatively, Cusumano and Bai [11] and Wagg and Bishop [65] applied a threshold on the time-interval between consecutive impacts to terminate chattering motion.

The motivation for this study is to bring forward (complete) chattering and its significance on rocking response, which has been rarely considered in rocking dynamics and earthquake engineering. Focusing on sinusoidal excitation, the specific aim is to determine the conditions under which chattering occurs, approximate how long it takes for chattering to complete (chattering time), and offer a glimpse into its implications on rocking dynamics. For this purpose, this study (i) adopts perturbation theory [34] and proposes, for the first time, an asymptotic approximation of chattering time for the rocking problem, (ii) demonstrates that within this (chattering) time-frame, the rocking block can come to rest even though the ground excitation is still active, and (iii) discusses implications of chattering using numerical simulations.

## 2 Dynamics of the rocking block

The rigid rocking block is an archetypal structural model that describes a wide class of rocking configurations [12], and a typical example of nonsmooth dynamics, in which smooth motion is interrupted by nonsmooth velocity "jumps", i.e. impacts [7, 25]. The present study focuses on the transient response of a rocking block when subjected to multi-lobe mathematical ground excitations of low amplitude and finite duration.

### 2.1 Rocking initiation

Consider the rigid block of Fig. 1 under a horizontal ground acceleration time-history $\ddot{u}_g$. Assuming the block does not slide at the contact interface and it is slender enough to avoid bouncing effects, rocking commences once the seismic demand, i.e. the moment of the inertia forces with respect to the pivot point O (or O′), exceeds the seismic resistance, i.e. the moment of the weight with respect to the same pivot point. This moment equilibrium condition yields the minimum ground

acceleration $a_{g,\min}$ necessary to initiate rocking.

$$\ddot{u}_g(t) \geq a_{g,\min} = g\tan\alpha \tag{1}$$

where $g$ denotes the gravitational acceleration, while $\alpha$ is the slenderness angle ($\alpha = \tan^{-1}(b/h)$) with $b$ being the block's half width and $h$ being the half height (Fig. 1). For slender structures, Eq. (1) becomes: $a_{g,\min} \approx g\alpha$.

### 2.2 Equations of motion and closed-form solutions

After rocking initiates, the continuous smooth motion of the block is interrupted by nonsmooth impacts at the pre-defined pivot (contact) points (Fig. 1). Moment equilibrium with respect to the pivot point O (or O′) yields the equations which describe the continuous smooth rocking motion of the block:

$$\begin{aligned} I_0\ddot{\theta} + mgR\sin(\alpha-\theta) &= -m\ddot{u}_g R\cos(\alpha-\theta), \qquad \theta > 0 \\ I_0\ddot{\theta} + mgR\sin(-\alpha-\theta) &= -m\ddot{u}_g R\cos(-\alpha-\theta), \quad \theta < 0 \end{aligned} \tag{2}$$

where $I_0$ represents the moment of inertia of the rigid body with respect to the pivot point O (or O′), $m$ is the mass of the block, $R$ is the half-diagonal distance measured from the pivot point to the centre of mass (C.M.), and $\theta$ is the rocking (rigid body) rotation (Fig. 1). Equation (2) is a set of ordinary differential equations that depends on the sign of $\theta$. For slender structures, Eq. (2) can be linearised to [17]:

$$\frac{\ddot{\theta}}{p^2\alpha} - \frac{\theta}{\alpha} + sgn(\theta) = -\frac{\ddot{u}_g}{g\alpha} \tag{3}$$

$p = \sqrt{3g/(4R)}$ in Eq. (3) denotes the frequency parameter of the block, while $sgn(\theta)$ is the standard sign function (i.e. $sgn(\theta) = 1$ when $\theta > 0$, $sgn(\theta) = 0$ when $\theta = 0$, and $sgn(\theta) = -1$ when $\theta < 0$). The dynamic behaviour of the rigid rocking block of Fig. 1 is described by the dimensionless equation of Eq. (3), which for a (harmonic) sinusoidal excitation can be written as [17]:

$$\phi_n''(\tau) - \phi_n(\tau) + sgn(\phi_n) = -a\sin(\omega\tau + \psi), \quad \tau \leq \tau_{ex} \tag{4}$$

where $\tau$ is the dimensionless time and $\tau_{ex}$ is the dimensionless time-instant at which the ground excitation ends, while $\psi$ is the phase angle when rocking commences. $\phi(\tau)$ is the dimensionless rotation at time $\tau$, and $\phi''(\tau)$ is the dimensionless angular acceleration at time $\tau$. $a$ is the dimensionless amplitude of the horizontal ground acceleration, and $\omega$ is the frequency ratio with $\omega_g$ being the frequency of the ground excitation:

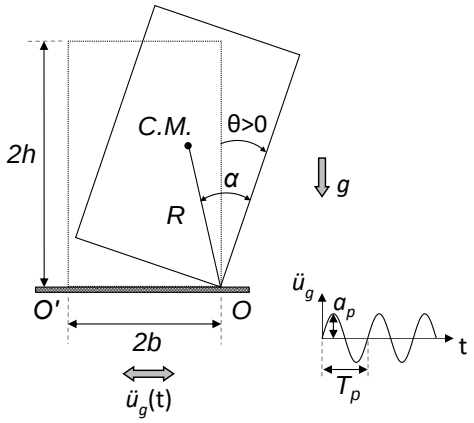


**Fig. 1** The archetypal rigid rocking block under horizontal ground excitation.

$$\begin{aligned} \phi_n'' &= \frac{\ddot{\theta}_n}{p^2\alpha}, & \phi_n &= \frac{\theta_n}{\alpha}, & \tau &= pt, \\ \omega &= \frac{\omega_g}{p}, & a &= \frac{\ddot{u}_g}{g\alpha} \end{aligned} \tag{5}$$

Subscript $n$ refers to the number of impacts that have already occurred during rocking motion.

Conveniently, Eq. (4) allows for an analytical solution, which can be expressed as [17]:

$$\begin{aligned} \phi_n(\tau) &= B_n e^{\tau} + A_n e^{-\tau} + i_n + \Xi(\tau) \\ \phi_n'(\tau) &= B_n e^{\tau} - A_n e^{-\tau} + \Xi'(\tau) \end{aligned} \tag{6}$$

with derivatives:

$$\begin{aligned} \phi_n''(\tau) &= B_n e^{\tau} + A_n e^{-\tau} + \Xi''(\tau) \\ \phi_n^{(3)}(\tau) &= B_n e^{\tau} - A_n e^{-\tau} + \Xi^{(3)}(\tau) \\ \phi_n^{(4)}(\tau) &= B_n e^{\tau} + A_n e^{-\tau} + \Xi^{(4)}(\tau) \\ \phi_n^{(5)}(\tau) &= B_n e^{\tau} - A_n e^{-\tau} + \Xi^{(5)}(\tau) \end{aligned} \tag{7}$$

where $A_n$, $B_n$ are terms that depend on the initial conditions. $i_n$ represents the sign of rocking rotation and is equal to $i_n = \pm 1$. Specifically, when the rocking block undergoes clockwise rotation $i_n = 1$, otherwise $i_n = -1$. Assuming the ground acceleration is initially positive, the initial rotation of the block is counter-clockwise, hence, without loss of generality, for $n = 0$ it follows $i_0 = -1$. The term $\Xi(\tau)$ represents the particular solution of the differential equation of Eq. (4), which captures the effect of the specific ground motion on rocking response. For a sinusoidal ground acceleration, $\Xi(\tau)$ takes the form [16]:

$$\begin{aligned} \Xi(\tau) &= \frac{1}{\omega^2+1} a\sin(\omega\tau + \psi) \\ \Xi'(\tau) &= \frac{\omega}{\omega^2+1} a\cos(\omega\tau + \psi) \end{aligned} \tag{8}$$

with derivatives:

$$\begin{aligned}\Xi^{''}(\tau) &= -\frac{\omega^2}{\omega^2+1}a\sin(\omega\tau+\psi)\\ \Xi^{(3)}(\tau) &= -\frac{\omega^3}{\omega^2+1}a\cos(\omega\tau+\psi)\\ \Xi^{(4)}(\tau) &= \frac{\omega^4}{\omega^2+1}a\sin(\omega\tau+\psi)\\ \Xi^{(5)}(\tau) &= \frac{\omega^5}{\omega^2+1}a\cos(\omega\tau+\psi)\end{aligned} \tag{9}$$

For $n=0$ and $\tau=\tau_0=0$, i.e. the time-instant rocking commences (Fig. 2(b)), the initial conditions of the rocking block of Fig. 1 are: $\phi_0(\tau_0)=0$ and $\phi_0^{'}(\tau_0)=0$. Hence, Eq. (6) gives [16]:

$$\begin{aligned}A_0 &= -\frac{1}{2}\left[\Xi(\tau_0)-\Xi^{'}(\tau_0)+i_0\right]\\ B_0 &= -\frac{1}{2}\left[\Xi(\tau_0)+\Xi^{'}(\tau_0)+i_0\right]\end{aligned} \tag{10}$$

where from Eq. (8) for $\tau=\tau_0=0$:

$$\begin{aligned}\Xi(\tau_0) &= \frac{1}{\omega^2+1}a\sin(\psi)\\ \Xi^{'}(\tau_0) &= \frac{\omega}{\omega^2+1}a\cos(\psi)\end{aligned} \tag{11}$$

In addition, the initial conditions of $\phi_0(\tau_0)=0$ and $\phi_0^{''}(\tau_0)=0$ using Eq. (4) give the phase angle when rocking initiates:

$$\psi=\sin^{-1}\left(\frac{-i_0}{a}\right) \tag{12}$$

### 2.3 Treatment of impact

Impact occurs whenever the rocking rotation switches sign ($\phi_n(\tau_n)=0$). Assuming pure rocking behaviour (i.e. no sliding and bouncing effects during rocking), the block, after impact, switches pivot point and continues its smooth rocking motion about the new pivot point. Due to the impulsive nature of impact, at $\tau=\tau_n$ when impact happens, an instantaneous decrease in velocity occurs (i.e., nonsmooth velocity "jump" [7, 25]). Hence, the angular velocities before ($\phi_{n-1}^{'}(\tau_n)$) and after ($\phi_n^{'}(\tau_n)$) impact are connected through the (dimensionless) coefficient of restitution $\eta$ [35].

$$\phi_n^{'}(\tau_n)=\eta\phi_{n-1}^{'}(\tau_n) \tag{13}$$

One way to analytically estimate the coefficient of restitution $\eta$ is via the conservation of moment of momentum, just before and just after impact [35]. Yet, this is merely a theoretical approximation, since the amount of (kinetic) energy lost at impact is not solely a function of the block's geometry (see e.g. [4, 20, 38] and references therein). Thus, the value of coefficient of restitution $\eta$ is usually inverse fitted from experiments [20] or assumed [27]. This study considers the coefficient of restitution an independent parameter able to incorporate any of the above modifications.

## 3 Asymptotic approximation of the chattering time

This section investigates the chattering behaviour of a rocking block under a low amplitude (i.e. weak) ground excitation. It specifically aims to approximate asymptotically the duration of chattering motion $\tau_{ch}$, namely the finite time the block takes to come to rest through a theoretically infinite sequence of impacts under weak ground excitation. The proposed asymptotic approach builds on the pioneering study of the inverted pendulum problem by Demeio and Lenci [13]. The rocking problem examined herein differs from the inverted pendulum as after every impact the equation of motion changes (as reflected in Eq. (6) by the value of $i_n$), which further complicates the proposed approach.

The premise of this asymptotic approach is that the chattering time is the total duration the sequence of impacts last till the block comes to rest. This duration equals the sum of the time-intervals $\Delta\tau$ between these infinite consecutive impacts (Fig. 2). The time-instant $\tau=\tau_{n+1}$ the $(n+1)^{th}$ impact occurs is determined from the expression of rocking rotation initiated after the $n^{th}$ impact $\phi_n(\tau_{n+1})=0$. To calculate $\tau_{n+1}$, one must first calculate the initial conditions of the cycle of motion after the $n^{th}$ impact. This necessitates the derivation of general expressions of the angular velocity $\phi_n^{'}(\tau_n)$ of the block at (any) impact $n$, and of the time-interval $\Delta\tau_n$ between consecutive impacts at $\tau_n$ and $\tau_{n+1}$. Accordingly, the approach treats separately the first cycle of rocking motion (Section 3.1) from all subsequent cycles of rocking motion (Sections 3.2, 3.3), as their initial conditions (and specifically the angular velocity) differ.

For the sake of analytical solutions, this section considers a (harmonic) sinusoidal ground excitation and adopts perturbation theory [34] to expand the rocking rotation $\phi_n(\tau)$ and the time-interval $\Delta\tau_n$ in power series of a small parameter $\varepsilon$. The parameter $\varepsilon$ relates to the dimensionless amplitude of the ground acceleration $a$:

$$a=\frac{\ddot{u}_g}{g\alpha}=\varepsilon+1 \tag{14}$$

Note that $a=1$ corresponds to $\varepsilon=0$ and represents the critical acceleration value above which ($a\geq 1$)

rocking commences (Eq. (1)). Specifically, a small positive $\varepsilon$ value indicates a weak ground excitation, barely capable of triggering rocking motion. Thus, the rocking problem examined herein is governed by the dimensionless acceleration amplitude $a$ and frequency $\omega$ of the ground excitation (Eq. (5)) and the dimensionless coefficient of restitution $\eta$ (Eq. (13)) that controls the energy dissipation at impact.

In this context, the rocking rotation can be written as [13]:

$$\phi_n(\tau) = \sum_{m=0}^{M} \Phi_n^{(m)} (\tau - \tau_n)^m \tag{15}$$

where

$$\Phi_n^{(m)} = \frac{1}{m!} \frac{d^m \phi_n}{d\tau^m}(\tau_n) \tag{16}$$

$m$ defines the order of time-derivative, while $n$ refers to the number of impacts. Equation (15), when the $(n+1)^{th}$ impact happens (i.e. at $\tau = \tau_{n+1}$), gives:

$$\sum_{m=0}^{M} \Phi_n^{(m)} (\Delta\tau_n)^m = 0 \tag{17}$$

where $\Delta\tau_n = \tau_{n+1} - \tau_n$ denotes the time-interval between two consecutive impacts that occur at the time-instants $\tau_n$ and $\tau_{n+1}$ (Fig. 2(c)). Using the definition of $\Phi_n^{(m)}$ (Eq. (16)), Eq. (17) reads:

$$\phi_n(\tau_n) + \sum_{m=1}^{M} \Phi_n^{(m)} (\Delta\tau_n)^m = 0 \tag{18}$$

where $\phi_n(\tau_n) = 0$ since impact happens. Hence, Eq. (18) becomes:

$$\Delta\tau_n \sum_{m=1}^{M} \Phi_n^{(m)} (\Delta\tau_n)^{m-1} = 0 \tag{19}$$

which implies that at the time-instant $\tau_{n+1}$ the $(n+1)^{th}$ impact happens ($\phi_n(\tau_{n+1}) = 0$):

$$\sum_{m=0}^{M-1} \Phi_n^{(m+1)} (\Delta\tau_n)^m = 0 \tag{20}$$

### 3.1 First cycle of rocking motion

This section approximates the angular velocity of the rocking block $\phi_0'(\tau_1)$ at the time-instant of the first impact $\tau = \tau_1$. To this end, it first approximates $\tau_1$, or equivalently $\Delta\tau_0 = \tau_1 - \tau_0$, from Eq. (20) for $n = 0$, namely $\phi_0(\tau_1) = 0$.

During the first cycle of rotation (i.e. $n = 0$ in Fig. 2(b)), Eq. (15) can be expanded in Taylor series centred at the time-instant $\tau_0 = 0$ rocking initiates:

$$\begin{aligned} \phi_0(\tau) &= \sum_{m=0}^{M} \Phi_0^{(m)} (\tau - \tau_0)^m \\ &= \sum_{m=0}^{M} \left[ \frac{1}{m!} \frac{d^m \phi_0}{d\tau^m}(\tau_0) \right] (\tau - \tau_0)^m \end{aligned} \tag{21}$$

Substituting Eqs (6), (7) with the aid of Eq. (10) into Eq. (21) and re-ordering the terms:

$$\begin{aligned} \phi_0(\tau) = &\frac{1}{3!} \left[ \Xi^{(3)}(\tau_0) - \Xi'(\tau_0) \right] (\tau - \tau_0)^3 \\ &+ \frac{1}{4!} \left[ \Xi^{(4)}(\tau_0) - \Xi''(\tau_0) \right] (\tau - \tau_0)^4 \\ &+ \frac{1}{5!} \left[ \Xi^{(5)}(\tau_0) - \Xi'(\tau_0) \right] (\tau - \tau_0)^5 + \ldots \end{aligned} \tag{22}$$

Equations (21), (22) give:

$$\begin{aligned} \Phi_0^{(0)} &= 0 \\ \Phi_0^{(1)} &= 0 \\ \Phi_0^{(2)} &= 0 \\ \Phi_0^{(3)} &= \frac{1}{3!} \left[ \Xi^{(3)}(\tau_0) - \Xi'(\tau_0) \right] \\ \Phi_0^{(4)} &= \frac{1}{4!} \left[ \Xi^{(4)}(\tau_0) - \Xi''(\tau_0) \right] \\ \Phi_0^{(5)} &= \frac{1}{5!} \left[ \Xi^{(5)}(\tau_0) - \Xi'(\tau_0) \right] \end{aligned} \tag{23}$$

Equation (23) implies that, at $\tau_0 = 0$, the rotation $\Phi_0^{(0)}$, the angular velocity $\Phi_0^{(1)}$, and the angular acceleration $\Phi_0^{(2)}$ are zero. The angular jerk $\Phi_0^{(3)}$ is nonzero as it describes the rate of change of the angular acceleration at the time-instant rocking initiates. The $\Xi^{(m)}(\tau_0)$ terms in Eq. (23) are related to the forcing function (Eqs (8), (9)). Because of Eq. (14), the trigonometric terms of Eqs (8), (9), (11) become:

$$\begin{aligned} a\sin(\omega\tau_0 + \psi) &= a\sin(\psi) = -i_0 \\ a\cos(\omega\tau_0 + \psi) &= a\cos(\psi) = \sqrt{2\varepsilon + \varepsilon^2} \end{aligned} \tag{24}$$

The second equation of Eq. (24) can be expanded in Taylor series in powers of $\varepsilon$:

$$\begin{aligned} a\cos(\omega\tau_0 + \psi) &= a\cos(\psi) \\ &= \sqrt{2} \left[ \varepsilon^{\frac{1}{2}} + \frac{\varepsilon^{\frac{3}{2}}}{4} - \frac{\varepsilon^{\frac{5}{2}}}{32} + O\left(\varepsilon^{\frac{7}{2}}\right) \right] \end{aligned} \tag{25}$$

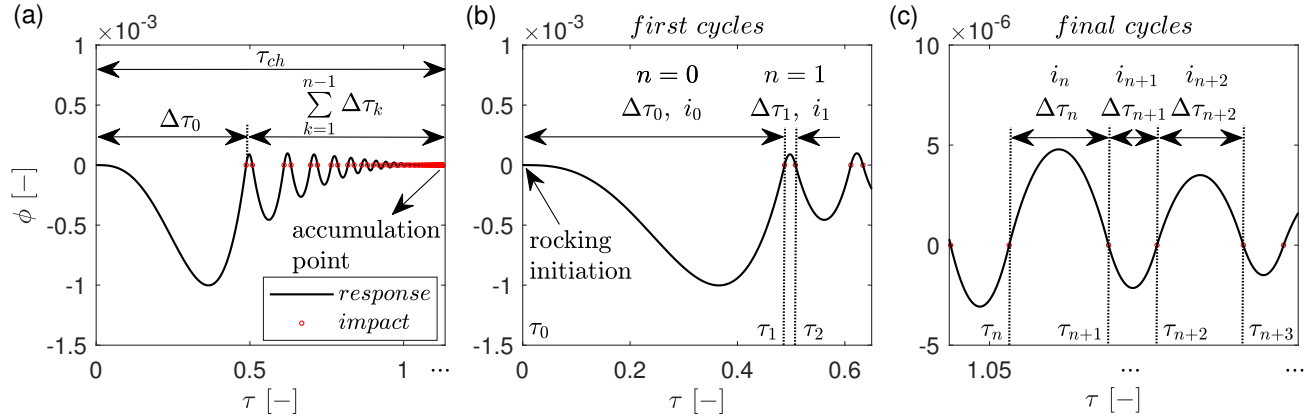


**Fig. 2** (a) Chattering oscillations of the rocking block ($p = 1\ s^{-1}$ and $\alpha = 0.2\ rad$) of Fig. 1 when subjected to a sinusoidal ground excitation of amplitude $a = 1.03$ and frequency $\omega = 2$ for $\eta = 0.92$, with details of the (b) first and (c) final response cycles.

Therefore, Eqs (8), (9) through Eqs (24), (25) for $\tau = \tau_0$ become:

$$
\begin{aligned}
\Xi(\tau_0) &= -\frac{i_0}{\omega^2+1} \\
\Xi'(\tau_0) &= \frac{\omega}{\omega^2+1}\sqrt{2}\left[\varepsilon^{\frac{1}{2}} + \frac{\varepsilon^{\frac{3}{2}}}{4} - \frac{\varepsilon^{\frac{5}{2}}}{32} + O\left(\varepsilon^{\frac{7}{2}}\right)\right] \\
\Xi''(\tau_0) &= \frac{\omega^2 i_0}{\omega^2+1} \\
\Xi^{(3)}(\tau_0) &= -\frac{\omega^3}{\omega^2+1}\sqrt{2}\left[\varepsilon^{\frac{1}{2}} + \frac{\varepsilon^{\frac{3}{2}}}{4} - \frac{\varepsilon^{\frac{5}{2}}}{32} + O\left(\varepsilon^{\frac{7}{2}}\right)\right] \\
\Xi^{(4)}(\tau_0) &= -\frac{\omega^4 i_0}{\omega^2+1} \\
\Xi^{(5)}(\tau_0) &= \frac{\omega^5}{\omega^2+1}\sqrt{2}\left[\varepsilon^{\frac{1}{2}} + \frac{\varepsilon^{\frac{3}{2}}}{4} - \frac{\varepsilon^{\frac{5}{2}}}{32} + O\left(\varepsilon^{\frac{7}{2}}\right)\right]
\end{aligned}
\tag{26}
$$

Subsequently, Eq. (23) through Eq. (26) reads:

$$
\begin{aligned}
\Phi_0^{(0)} &= 0 \\
\Phi_0^{(1)} &= 0 \\
\Phi_0^{(2)} &= 0 \\
\Phi_0^{(3)} &= -\frac{\omega}{6}\sqrt{2}\left[\varepsilon^{\frac{1}{2}} + \frac{\varepsilon^{\frac{3}{2}}}{4} - \frac{\varepsilon^{\frac{5}{2}}}{32} + O\left(\varepsilon^{\frac{7}{2}}\right)\right] \\
\Phi_0^{(4)} &= -\frac{\omega^2 i_0}{24} \\
\Phi_0^{(5)} &= \frac{\omega(\omega^2-1)}{120}\sqrt{2}\left[\varepsilon^{\frac{1}{2}} + \frac{\varepsilon^{\frac{3}{2}}}{4} - \frac{\varepsilon^{\frac{5}{2}}}{32} + O\left(\varepsilon^{\frac{7}{2}}\right)\right]
\end{aligned}
\tag{27}
$$

Observe that each order of time-derivative in Eq. (27) can be expressed in the general form:

$$
\begin{aligned}
\Phi_0^{(m)} &= \Phi_{0;0}^{(m)} + \Phi_{0;1}^{(m)}\varepsilon^{\frac{1}{2}} + \Phi_{0;3}^{(m)}\varepsilon^{\frac{3}{2}} + \Phi_{0;5}^{(m)}\varepsilon^{\frac{5}{2}} + O\left(\varepsilon^{\frac{7}{2}}\right) \\
&= \Phi_{0;0}^{(m)} + \sum_{l=0}^{L} \Phi_{0;2l+1}^{(m)}\varepsilon^{\frac{2l+1}{2}}
\end{aligned}
\tag{28}
$$

where, the superscript $m$ of e.g. $\Phi_{0;1}^{(m)}$ indicates the order of differentiation, and the subscript "0;1" of $\Phi_{0;1}^{(m)}$ represents the number of impacts with the first subscript "0", and the order of approximation $l$ in powers of $\varepsilon$ with the second subscript "1". The expansion of $\Phi_0^{(m)}$ in half-integer powers of $\varepsilon$ (Eqs (27), (28)) suggests an expansion of $\Delta\tau_0$ (Fig. 2(b)) also in half-integer powers of $\varepsilon$:

$$
\begin{aligned}
\Delta\tau_0 &= \tau_1 - \tau_0 \\
&= T_{0;0} + T_{0;1}\varepsilon^{\frac{1}{2}} + T_{0;2}\varepsilon^{\frac{2}{2}} + T_{0;3}\varepsilon^{\frac{3}{2}} + O\left(\varepsilon^{\frac{4}{2}}\right)
\end{aligned}
\tag{29}
$$

Expanding Eq. (20) for $n = 0$ and using Eqs (28), (29):

$$
\begin{aligned}
&\Phi_{0;0}^{(4)}T_{0;0} + \left[\Phi_{0;1}^{(3)} + \Phi_{0;0}^{(4)}T_{0;1} + \Phi_{0;1}^{(5)}(T_{0;0})^2\right]\varepsilon^{\frac{1}{2}} \\
&+ \left[\Phi_{0;0}^{(4)}T_{0;2} + 2\Phi_{0;1}^{(5)}T_{0;0}T_{0;1}\right]\varepsilon^{\frac{2}{2}} \\
&+ \begin{bmatrix}\Phi_{0;3}^{(3)} + \Phi_{0;0}^{(4)}T_{0;3} + \Phi_{0;1}^{(5)}{T_{0;1}}^2 \\ +2\Phi_{0;1}^{(5)}T_{0;0}T_{0;2} + \Phi_{0;3}^{(5)}{T_{0;0}}^2\end{bmatrix}\varepsilon^{\frac{3}{2}} + O\left(\varepsilon^{\frac{4}{2}}\right) = 0
\end{aligned}
\tag{30}
$$

Equation (30) yields a hierarchy of equations in powers of $\varepsilon$, the solution of which returns the terms of Eq. (29):

$$\begin{aligned}
&\varepsilon^{\frac{0}{2}}:\ T_{0;0}=0\\
&\varepsilon^{\frac{1}{2}}:\ T_{0;1}=-\frac{4\sqrt{2}}{\omega i_0}\\
&\varepsilon^{\frac{2}{2}}:\ T_{0;2}=0\\
&\varepsilon^{\frac{3}{2}}:\ T_{0;3}=\frac{\sqrt{2}}{\omega i_0}\left[-1+\frac{32\left(\omega^2-1\right)}{5\omega^2}\right]
\end{aligned} \tag{31}$$

Hence, the time-instant the first impact happens becomes (Eq. (29)):

$$\tau_1=-\frac{4\sqrt{2}}{\omega i_0}\varepsilon^{\frac{1}{2}}+\frac{\sqrt{2}}{\omega i_0}\left[-1+\frac{32\left(\omega^2-1\right)}{5\omega^2}\right]\varepsilon^{\frac{3}{2}}+O\left(\varepsilon^{\frac{4}{2}}\right) \tag{32}$$

Differentiation of Eq. (15) for $\tau=\tau_1$ and $n=0$ gives the angular velocity at first impact ($\tau_1$):

$$\phi_0^{'}\left(\tau_1\right)=\sum_{m=0}^{M-1}(\mathrm{m}+1)\Phi_0^{(m+1)}(\Delta\tau_0)^m \tag{33}$$

Substituting Eqs (27), (29) into the expanded form of Eq. (33) returns the angular velocity at first impact ($\tau_1$):

$$\phi_0^{'}\left(\tau_1\right)=\frac{16\sqrt{2}}{3\omega}\varepsilon^{\frac{3}{2}}+\frac{4\sqrt{2}}{\omega}\left[1-\frac{32\left(\omega^2-1\right)}{15\omega^2}\right]\varepsilon^{\frac{5}{2}}+O\left(\varepsilon^{\frac{7}{2}}\right) \tag{34}$$

from which, based on Eq. (28):

$$\begin{aligned}
&\varepsilon^{\frac{0}{2}}:\ \Phi_{0;0}^{(1)}=0\\
&\varepsilon^{\frac{1}{2}}:\ \Phi_{0;1}^{(1)}=0\\
&\varepsilon^{\frac{3}{2}}:\ \Phi_{0;3}^{(1)}=\frac{16\sqrt{2}}{3\omega}\\
&\varepsilon^{\frac{5}{2}}:\ \Phi_{0;5}^{(1)}=\frac{4\sqrt{2}}{\omega}\left[1-\frac{32\left(\omega^2-1\right)}{15\omega^2}\right]
\end{aligned} \tag{35}$$

Therefore, the angular velocity of the rocking block after the first impact is given from the angular velocity before impact (Eq. (34)) with the aid of the coefficient of restitution $\eta$ (Eq. (13)): $\phi_1^{'}\left(\tau_1\right)=\eta\phi_0^{'}\left(\tau_1\right)$.

### 3.2 Subsequent cycles of rocking motion

For all subsequent impacts, the calculation steps are similar as in Section 3.1 with the main difference being the initial conditions (and specifically the angular velocity) after each impact. In particular, after the first impact (i.e. $n=1$ in Fig. 2(b)) at $\tau=\tau_1$, the new initial conditions $\phi_1\left(\tau_1\right)=0$ and $\phi_1^{'}\left(\tau_1\right)\neq 0$ according to Eq. (6) give:

$$\begin{aligned}
&B_1e^{\tau_1}+A_1e^{-\tau_1}=-i_1-\Xi\left(\tau_1\right)\\
&B_1e^{\tau_1}-A_1e^{-\tau_1}=\phi_1^{'}\left(\tau_1\right)-\Xi^{'}\left(\tau_1\right)
\end{aligned} \tag{36}$$

in which $i_1=-i_0$, as the sign of rotation after the first impact changes (Fig. 2(b)). Equation (15) for $n=1$ becomes:

$$\begin{aligned}
\phi_1\left(\tau\right)&=\sum_{m=0}^{M}\Phi_1^{(m)}(\tau-\tau_1)^m\\
&=\sum_{m=0}^{M}\left[\frac{1}{m!}\frac{d^m\phi_1}{d\tau^m}\left(\tau_1\right)\right](\tau-\tau_1)^m
\end{aligned} \tag{37}$$

Expansion of Eq. (37) considering Eqs (6), (7), (36) yields:

$$\begin{aligned}
\phi_1\left(\tau\right)=&\frac{1}{1!}\phi_1^{'}\left(\tau_1\right)\left(\tau-\tau_1\right)\\
&+\frac{1}{2!}\left[-i_1-\Xi\left(\tau_1\right)+\Xi^{''}\left(\tau_1\right)\right]\left(\tau-\tau_1\right)^2\\
&+\frac{1}{3!}\left[\phi_1^{'}\left(\tau_1\right)-\Xi^{'}\left(\tau_1\right)+\Xi^{(3)}\left(\tau_1\right)\right]\left(\tau-\tau_1\right)^3\\
&+\frac{1}{4!}\left[-i_1-\Xi\left(\tau_1\right)+\Xi^{(4)}\left(\tau_1\right)\right]\left(\tau-\tau_1\right)^4+...
\end{aligned} \tag{38}$$

Equations (37), (38) give:

$$\begin{aligned}
&\Phi_1^{(0)}=0\\
&\Phi_1^{(1)}=\phi_1^{'}\left(\tau_1\right)\\
&\Phi_1^{(2)}=\frac{1}{2!}\left[-i_1-\Xi\left(\tau_1\right)+\Xi^{''}\left(\tau_1\right)\right]\\
&\Phi_1^{(3)}=\frac{1}{3!}\left[\phi_1^{'}\left(\tau_1\right)-\Xi^{'}\left(\tau_1\right)+\Xi^{(3)}\left(\tau_1\right)\right]\\
&\Phi_1^{(4)}=\frac{1}{4!}\left[-i_1-\Xi\left(\tau_1\right)+\Xi^{(4)}\left(\tau_1\right)\right]
\end{aligned} \tag{39}$$

Alternatively, Eq. (39) for $n=1$ can be expressed as:

$$\begin{aligned}
\Phi_1^{(2m+1)}&=\frac{1}{(2m+1)!}\left[\phi_1^{'}\left(\tau_1\right)-\Xi^{(1)}\left(\tau_1\right)+\Xi^{(2m+1)}\left(\tau_1\right)\right]\\
\Phi_1^{(2m)}&=\frac{1}{(2m)!}\left[-i_1-\Xi\left(\tau_1\right)+\Xi^{(2m)}\left(\tau_1\right)\right]
\end{aligned} \tag{40}$$

Thus, in general, for any impact $n$, Eq. (40) becomes:

$$\begin{aligned}
\Phi_n^{(2m+1)}&=\frac{1}{(2m+1)!}\begin{bmatrix}\phi_n^{'}\left(\tau_n\right)-\Xi^{(1)}\left(\tau_n\right)\\+\Xi^{(2m+1)}\left(\tau_n\right)\end{bmatrix},\quad m\geq 0\\
\Phi_n^{(2m)}&=\frac{1}{(2m)!}\left[-i_n-\Xi\left(\tau_n\right)+\Xi^{(2m)}\left(\tau_n\right)\right],\quad m>0
\end{aligned} \tag{41}$$

### 3.3 Chattering time

As the rocking block continues its chattering oscillations subjected to ground excitation, its velocity lessens at every impact till it eventually becomes zero after a theoretically infinite number of impacts (Fig. 2(a)). This section approximates the time needed for the block to come to rest, i.e. chattering time, while subjected to a nonzero (weak) ground excitation.

The chattering time is equal with the total duration of the sequence of impacts (Fig. 2(a)):

$$\tau_{ch} = \sum_{n=0}^{\infty} \Delta\tau_n \tag{42}$$

where $n$ represents the number of impacts. Following Eq. (29), $\Delta\tau_n$ can be expanded as:

$$\begin{aligned}\Delta\tau_n &= \tau_{n+1} - \tau_n \\ &= T_{n;0} + T_{n;1}\varepsilon^{\frac{1}{2}} + T_{n;2}\varepsilon^{\frac{2}{2}} + T_{n;3}\varepsilon^{\frac{3}{2}} + O\left(\varepsilon^{\frac{4}{2}}\right) \\ &= \sum_{l=0}^{L} T_{n;l}\varepsilon^{\frac{l}{2}}\end{aligned} \tag{43}$$

where, again, $l$ refers to the order of approximation. Thus, at any time-instant of impact $\phi_n(\tau_n) = 0$, Eq. (20) gives:

$$\Phi_n^{(1)} + \Phi_n^{(2)}\Delta\tau_n + \Phi_n^{(3)}(\Delta\tau_n)^2 + \Phi_n^{(4)}(\Delta\tau_n)^3 + ... = 0 \tag{44}$$

Recall that the term $\Phi_n^{(m)}$ in Eq. (44) represents the $m^{th}$ derivative of rocking rotation after the $n^{th}$ impact and is given by Eq. (41) as:

$$\begin{aligned}\Phi_n^{(1)} &= \phi_n^{'}(\tau_n) \\ \Phi_n^{(2)} &= \frac{1}{2}\left[-i_n - \Xi(\tau_n) + \Xi^{(2)}(\tau_n)\right] \\ \Phi_n^{(3)} &= \frac{1}{6}\left[\phi_n^{'}(\tau_n) - \Xi^{(1)}(\tau_n) + \Xi^{(3)}(\tau_n)\right] \\ \Phi_n^{(4)} &= \frac{1}{24}\left[-i_n - \Xi(\tau_n) + \Xi^{(4)}(\tau_n)\right]\end{aligned} \tag{45}$$

The $\Phi_n^{(m)}$ terms in Eq. (45) rely on the general form of the forcing function $\Xi^{(m)}(\tau_n)$ (Eqs (8), (9)):

$$\begin{aligned}\Xi^{(2m)}(\tau_n) &= \frac{\omega^{2m}(-1)^m}{\omega^2+1} a\sin(\omega\tau_n + \psi) \\ \Xi^{(2m+1)}(\tau_n) &= \frac{\omega^{2m+1}(-1)^m}{\omega^2+1} a\cos(\omega\tau_n + \psi)\end{aligned} \tag{46}$$

and the time-instant the $n^{th}$ impact occurs $\tau_n$:

$$\begin{aligned}\tau_n = \tau_0 + \sum_{k=0}^{n-1}\Delta\tau_k &= \tau_0 + \sum_{l=1}^{L}\left(\sum_{k=0}^{n-1} T_{k;l}\right)\varepsilon^{\frac{l}{2}} \\ &= \tau_0 + \sum_{l=1}^{L}\sigma_{n;l}\varepsilon^{\frac{l}{2}}\end{aligned} \tag{47}$$

where $\sigma_{n;l}$ represents the summation of the $l^{th}$ order of approximation $T_{k;l}$ of all the the time-intervals $\Delta\tau_k$ between consecutive impacts.

$$\sigma_{n;l} = \sum_{k=0}^{n-1} T_{k;l} \tag{48}$$

with $\sigma_{n;0} = 0$ since $T_{n;0} = 0$ (Eq. (31)).

Using Eqs (47), (48), the trigonometric terms $\sin(\omega\tau_n + \psi)$, $\cos(\omega\tau_n + \psi)$ become:

$$\begin{aligned}\sin(\omega\tau_n + \psi) &= \sin\left[(\omega\tau_0 + \psi) + \omega\sum_{l=1}^{L}\sigma_{n;l}\varepsilon^{\frac{l}{2}}\right] \\ \cos(\omega\tau_n + \psi) &= \cos\left[(\omega\tau_0 + \psi) + \omega\sum_{l=1}^{L}\sigma_{n;l}\varepsilon^{\frac{l}{2}}\right]\end{aligned} \tag{49}$$

Series expansion of Eq. (49) gives [13]:

$$\begin{aligned}\sin\left[(\omega\tau_0 + \psi) + \omega\sum_{l=1}^{L}\sigma_{n;l}\varepsilon^{\frac{l}{2}}\right] &= \sum_{l=0}^{L} d_{n;l}\varepsilon^{\frac{l}{2}} \\ \cos\left[(\omega\tau_0 + \psi) + \omega\sum_{l=1}^{L}\sigma_{n;l}\varepsilon^{\frac{l}{2}}\right] &= \sum_{l=0}^{L} c_{n;l}\varepsilon^{\frac{l}{2}}\end{aligned} \tag{50}$$

where:

$$\begin{aligned}d_{n;0} &= -\frac{i_0}{a} \\ d_{n;1} &= 0 \\ d_{n;2} &= \frac{\sqrt{2}}{a}\omega\sigma_{n;1} + \frac{i_0}{2a}(\omega\sigma_{n;1})^2 \\ d_{n;3} &= 0 \\ c_{n;0} &= 0 \\ c_{n;1} &= \frac{\sqrt{2}}{a} + \frac{i_0}{a}\omega\sigma_{n;1} \\ c_{n;2} &= 0 \\ c_{n;3} &= \frac{\sqrt{2}}{4a} - \frac{\sqrt{2}}{2a}(\omega\sigma_{n;1})^2 - \frac{i_0}{6a}(\omega\sigma_{n;1})^3\end{aligned} \tag{51}$$

Recall that $\sigma_{n;1}$ represents the summation of the first order of approximation of all the time-intervals $\Delta\tau_n$ between consecutive impacts (Eq. (48)). Substituting Eqs (46), (49), (50) into Eq. (45):

$$\begin{aligned}\Phi_n^{(1)} &= \phi_n^{'}(\tau_n) \\ \Phi_n^{(2)} &= -\frac{i_n + a d_{n;0}}{2} - \frac{a}{2}d_{n;2}\varepsilon^{\frac{2}{2}} + O\left(\varepsilon^{\frac{4}{2}}\right) \\ \Phi_n^{(3)} &= \frac{1}{6}\Phi_n^{(1)} - \frac{a\omega}{6}c_{n;1}\varepsilon^{\frac{1}{2}} - \frac{a\omega}{6}c_{n;3}\varepsilon^{\frac{3}{2}} + O\left(\varepsilon^{\frac{4}{2}}\right) \\ \Phi_n^{(4)} &= \frac{-i_n + a\left(\omega^2 - 1\right)d_{n;0}}{24} + \frac{a\left(\omega^2-1\right)}{24}d_{n;2}\varepsilon^{\frac{2}{2}} + O\left(\varepsilon^{\frac{4}{2}}\right)\end{aligned} \tag{52}$$

The post-impact angular velocity $\phi_n^{'}(\tau_n)$ is connected to the pre-impact angular velocity $\phi_{n-1}^{'}(\tau_n)$ through the coefficient of restitution $\eta$ (Eq. (13)). Using the general form of Eq. (33):

$$\begin{aligned}\Phi_n^{(1)} &= \phi_n^{'}(\tau_n) = \eta\phi_{n-1}^{'}(\tau_n) \\ &= \eta\sum_{m=0}^{M-1}(m+1)\,\Phi_{n-1}^{(m+1)}(\tau_n-\tau_{n-1})^m\end{aligned} \tag{53}$$

Expanding Eq. (53) and using Eq. (52), the angular velocity at any impact $n$ becomes:

$$\Phi_n^{(1)} = \eta\left[\begin{array}{l}\Phi_{n-1}^{(1)} + 2\Phi_{n-1;0}^{(2)}T_{n-1;1}\varepsilon^{\frac{1}{2}} + \left(2\Phi_{n-1;0}^{(2)}T_{n-1;2} + \frac{1}{2}\Phi_{n-1}^{(1)}\left(T_{n-1;1}\right)^2\right)\varepsilon^{\frac{2}{2}} \\ + \left(\begin{array}{l}2\Phi_{n-1;2}^{(2)}T_{n-1;1} + 3\Phi_{n-1;1}^{(3)}\left(T_{n-1;1}\right)^2 + 2\Phi_{n-1;0}^{(2)}T_{n-1;3} \\ +\Phi_{n-1}^{(1)}T_{n-1;1}T_{n-1;2} + 4\Phi_{n-1;0}^{(4)}\left(T_{n-1;1}\right)^3\end{array}\right)\varepsilon^{\frac{3}{2}} + O\left(\varepsilon^{\frac{4}{2}}\right)\end{array}\right] \tag{54}$$

Recall that, based on Eq. (34), the lowest order of approximation of the angular velocity at the first impact ($\tau_1$) is $\varepsilon^{\frac{3}{2}}$. However, the lowest order of approximation of the angular velocity at the subsequent impacts ($\Phi_{n-1}^{(1)}$ for $n>1$) remains unknown. Assuming that the lowest order of approximation of the angular velocity $\Phi_{n-1}^{(1)}$ is $\varepsilon^{\frac{1}{2}}$, Eq. (54) can be re-written as:

$$\Phi_n^{(1)} = \eta\left[\begin{array}{l}\left(\Phi_{n-1;1}^{(1)} + 2\Phi_{n-1;0}^{(2)}T_{n-1;1}\right)\varepsilon^{\frac{1}{2}} + \left(\Phi_{n-1;2}^{(1)} + 2\Phi_{n-1;0}^{(2)}T_{n-1;2}\right)\varepsilon^{\frac{2}{2}} \\ + \left(\begin{array}{l}\Phi_{n-1;3}^{(1)} + 2\Phi_{n-1;0}^{(2)}T_{n-1;3} + 2\Phi_{n-1;2}^{(2)}T_{n-1;1} \\ +\frac{1}{2}\Phi_{n-1;1}^{(1)}\left(T_{n-1;1}\right)^2 + 3\Phi_{n-1;1}^{(3)}\left(T_{n-1;1}\right)^2 + 4\Phi_{n-1;0}^{(4)}\left(T_{n-1;1}\right)^3\end{array}\right)\varepsilon^{\frac{3}{2}} + O\left(\varepsilon^{\frac{4}{2}}\right)\end{array}\right] \tag{55}$$

Equation (55) shows that the angular velocity $\Phi_n^{(1)}$ at any impact $n$ takes the general form:

$$\begin{aligned}\Phi_n^{(1)} &= \Phi_{n;1}^{(1)}\varepsilon^{\frac{1}{2}} + \Phi_{n;2}^{(1)}\varepsilon^{\frac{2}{2}} + \Phi_{n;3}^{(1)}\varepsilon^{\frac{3}{2}} + O\left(\varepsilon^{\frac{4}{2}}\right) \\ &= \sum_{l=0}^{L}\Phi_{n;l}^{(m)}\varepsilon^{\frac{l}{2}}\end{aligned} \tag{56}$$

with:

$$\begin{aligned}\Phi_{n;1}^{(1)} &= \eta\left(\Phi_{n-1;1}^{(1)} + 2\Phi_{n-1;0}^{(2)}T_{n-1;1}\right) \\ \Phi_{n;2}^{(1)} &= \eta\left(\Phi_{n-1;2}^{(1)} + 2\Phi_{n-1;0}^{(2)}T_{n-1;2}\right) \\ \Phi_{n;3}^{(1)} &= \eta\left(\begin{array}{l}\Phi_{n-1;3}^{(1)} + 2\Phi_{n-1;0}^{(2)}T_{n-1;3} + 2\Phi_{n-1;2}^{(2)}T_{n-1;1} \\ +\frac{1}{2}\Phi_{n-1;1}^{(1)}\left(T_{n-1;1}\right)^2 + 3\Phi_{n-1;1}^{(3)}\left(T_{n-1;1}\right)^2 \\ +4\Phi_{n-1;0}^{(4)}\left(T_{n-1;1}\right)^3\end{array}\right)\end{aligned} \tag{57}$$

where e.g. $\Phi_{n;2}^{(1)}$ represents the first derivative of rocking rotation (superscript $m=1$) for the second order of approximation (subscript after the semicolon $l=2$) after the $n^{th}$ impact (subscript before the semicolon). Equations (55), (57) also imply that the orders of approximation of the pre-impact angular velocity at the end of any cycle of rotation (i.e. at $\tau=\tau_{n+1}$) are related with the pertinent orders of approximation of the post-impact angular velocity at the beginning of that cycle of rotation (i.e. at $\tau=\tau_n$):

$$\begin{aligned}\Phi_{n;1}^{(1)}\Big|_{\tau_{n+1}} &= \Phi_{n;1}^{(1)}\Big|_{\tau_n} + 2\Phi_{n;0}^{(2)}\Big|_{\tau_n}T_{n;1} \\ \Phi_{n;2}^{(1)}\Big|_{\tau_{n+1}} &= \Phi_{n;2}^{(1)}\Big|_{\tau_n} + 2\Phi_{n;0}^{(2)}\Big|_{\tau_n}T_{n;2} \\ \Phi_{n;3}^{(1)}\Big|_{\tau_{n+1}} &= \Phi_{n;3}^{(1)}\Big|_{\tau_n} + 2\Phi_{n;0}^{(2)}\Big|_{\tau_n}T_{n;3} \\ &\quad + 2\Phi_{n;2}^{(2)}\Big|_{\tau_n}T_{n;1} + \frac{1}{2}\Phi_{n;1}^{(1)}\Big|_{\tau_n}\left(T_{n;1}\right)^2 \\ &\quad + 3\Phi_{n;1}^{(3)}\Big|_{\tau_n}\left(T_{n;1}\right)^2 + 4\Phi_{n;0}^{(4)}\Big|_{\tau_n}\left(T_{n;1}\right)^3\end{aligned} \tag{58}$$

Equation (58) verifies Eq. (35) for $n = 0$. Therefore, Eq. (52) can be expressed in the general form:

$$\begin{aligned}
\Phi_n^{(1)} &= \Phi_{n;1}^{(1)}\varepsilon^{\frac{1}{2}} + \Phi_{n;2}^{(1)}\varepsilon^{\frac{2}{2}} + \Phi_{n;3}^{(1)}\varepsilon^{\frac{3}{2}} + O\left(\varepsilon^{\frac{4}{2}}\right) \\
\Phi_n^{(2)} &= \Phi_{n;0}^{(2)} + \Phi_{n;2}^{(2)}\varepsilon^{\frac{2}{2}} + O\left(\varepsilon^{\frac{4}{2}}\right) \\
\Phi_n^{(3)} &= \frac{1}{6}\left(\Phi_{n;1}^{(1)}\varepsilon^{\frac{1}{2}} + \Phi_{n;2}^{(1)}\varepsilon^{\frac{2}{2}} + \Phi_{n;3}^{(1)}\varepsilon^{\frac{3}{2}}\right) \\
&\quad + \Phi_{n;1}^{(3)}\varepsilon^{\frac{1}{2}} + \Phi_{n;3}^{(3)}\varepsilon^{\frac{3}{2}} + O\left(\varepsilon^{\frac{4}{2}}\right) \\
\Phi_n^{(4)} &= \Phi_{n;0}^{(4)} + \Phi_{n;2}^{(4)}\varepsilon^{\frac{2}{2}} + O\left(\varepsilon^{\frac{4}{2}}\right)
\end{aligned} \tag{59}$$

where:

$$\begin{aligned}
\Phi_{n;0}^{(2)} &= -\frac{i_n + a d_{n;0}}{2}, & \Phi_{n;2}^{(2)} &= -\frac{a}{2} d_{n;2} \\
\Phi_{n;1}^{(3)} &= -\frac{a\omega}{6} c_{n;1}, & \Phi_{n;3}^{(3)} &= -\frac{a\omega}{6} c_{n;3} \\
\Phi_{n;0}^{(4)} &= \frac{-i_n + a\left(\omega^2 - 1\right) d_{n;0}}{24}, & \Phi_{n;2}^{(4)} &= \frac{a\left(\omega^2 - 1\right)}{24} d_{n;2}
\end{aligned} \tag{60}$$

Substituting Eqs (43), (59) into Eq. (44):

$$\begin{aligned}
&\left[\Phi_{n;1}^{(1)} + \Phi_{n;0}^{(2)} T_{n;1}\right]\varepsilon^{\frac{1}{2}} + \left[\Phi_{n;2}^{(1)} + \Phi_{n;0}^{(2)} T_{n;2}\right]\varepsilon^{\frac{2}{2}} \\
&+ \begin{bmatrix} \Phi_{n;3}^{(1)} + \Phi_{n;0}^{(2)} T_{n;3} + \Phi_{n;2}^{(2)} T_{n;1} \\ +\frac{1}{6}\Phi_{n;1}^{(1)}\left(T_{n;1}\right)^2 + \Phi_{n;1}^{(3)}\left(T_{n;1}\right)^2 \\ +\Phi_{n;0}^{(4)}\left(T_{n;1}\right)^3 \end{bmatrix}\varepsilon^{\frac{3}{2}} + O\left(\varepsilon^{\frac{4}{2}}\right) = 0
\end{aligned} \tag{61}$$

Equation (61) yields a hierarchy of equations in powers of $\varepsilon$. Observe from Eqs (60), (51) that $\Phi_{n;0}^{(2)}$ and $\Phi_{n;0}^{(4)}$ take different form based on the sign of rotation $i_n$ (e.g. $i_n = i_0$ or $i_n = -i_0$), which, subsequently, governs the form of Eq. (61). Accordingly, there is a need to examine two cases: $i_n = i_0$ and $i_n = -i_0$.

***Rotation of same sign as the sign of initial rotation ($i_n = i_0$)***

When the sign of rotation $i_n$ of the block after the $n^{th}$ impact is the same as the sign of the initial rotation $i_0$ (Fig. 2), $\Phi_{n;0}^{(2)} = 0$ (Eq. (60)) and thus solution of Eq. (61) for each order of $\varepsilon$ gives:

$$\begin{aligned}
&\varepsilon^{\frac{1}{2}} : \Phi_{n;1}^{(1)} = 0 \\
&\varepsilon^{\frac{2}{2}} : \Phi_{n;2}^{(1)} = 0 \\
&\varepsilon^{\frac{3}{2}} : \Phi_{n;0}^{(4)}\left(T_{n;1}\right)^3 + \Phi_{n;1}^{(3)}\left(T_{n;1}\right)^2 + \Phi_{n;2}^{(2)} T_{n;1} + \Phi_{n;3}^{(1)} = 0
\end{aligned} \tag{62}$$

where $\Phi_{n;0}^{(4)}, \Phi_{n;1}^{(3)}$ and $\Phi_{n;2}^{(2)}$ are given by Eq. (60), while $\Phi_{n;3}^{(1)}$ by Eq. (57). The first two equations of Eq. (62) verify the result of Eq. (27) for $n = 0$. Furthermore, the cubic equation of Eq. (62) has only one real positive root $T_{n;1}$, which represents the lowest order of approximation of the chattering time when $i_n = i_0$.

***Rotation of opposite sign to the sign of initial rotation ($i_n = -i_0$)***

When the sign of rotation $i_n$ of the block after the $n^{th}$ impact is opposite to the sign of the initial rotation $i_0$ (Fig. 2), $\Phi_{n;0}^{(2)} \neq 0$ (Eq. (60)) and thus solution of Eq. (61) for each order of $\varepsilon$ gives:

$$\begin{aligned}
&\varepsilon^{\frac{1}{2}} : T_{n;1} = -\frac{\Phi_{n;1}^{(1)}}{\Phi_{n;0}^{(2)}} \\
&\varepsilon^{\frac{2}{2}} : T_{n;2} = -\frac{\Phi_{n;2}^{(1)}}{\Phi_{n;0}^{(2)}} \\
&\varepsilon^{\frac{3}{2}} : T_{n;3} = -\frac{\begin{pmatrix} \Phi_{n;3}^{(1)} + \Phi_{n;2}^{(2)} T_{n;1} + \frac{1}{6}\Phi_{n;1}^{(1)}\left(T_{n;1}\right)^2 \\ +\Phi_{n;1}^{(3)}\left(T_{n;1}\right)^2 + \Phi_{n;0}^{(4)}\left(T_{n;1}\right)^3 \end{pmatrix}}{\Phi_{n;0}^{(2)}}
\end{aligned} \tag{63}$$

where $\Phi_{n;1}^{(1)}$, $\Phi_{n;2}^{(1)}$ and $\Phi_{n;3}^{(1)}$ are given by Eq. (57), while $\Phi_{n;2}^{(2)}$, $\Phi_{n;1}^{(3)}$ and $\Phi_{n;0}^{(4)}$ by Eq. (60). Note that, due to Eqs (62), (60), Eq. (57) returns $\Phi_{n;1}^{(1)} = 0$ and $\Phi_{n;2}^{(1)} = 0$. Therefore, Eq. (63) simplifies:

$$\begin{aligned}
&\varepsilon^{\frac{1}{2}} : T_{n;1} = 0 \\
&\varepsilon^{\frac{2}{2}} : T_{n;2} = 0 \\
&\varepsilon^{\frac{3}{2}} : T_{n;3} = -\frac{\Phi_{n;3}^{(1)}}{\Phi_{n;0}^{(2)}}
\end{aligned} \tag{64}$$

The third equation of Eq. (64) yields the lowest order of approximation of the chattering time when $i_n = -i_0$.

***Chattering time approximation***

Assuming that the lowest orders of approximation, namely $T_{n;1}$ given by solution of the cubic equation of Eq. (62) when $i_n = i_0$ and $T_{n;3}$ given by solution of Eq. (64) when $i_n = -i_0$, are sufficient, the approximated chattering time that brings the block to rest can be expressed as:

$$\tau_{ch} = \sum_{n=0}^{\infty} \Delta\tau_n \sim \underbrace{\sum_{n=2k}^{\infty} T_{n;1}\varepsilon^{\frac{1}{2}}}_{i_n = i_0} + \underbrace{\sum_{n=2k+1}^{\infty} T_{n;3}\varepsilon^{\frac{3}{2}}}_{i_n = -i_0} \tag{65}$$

where $k$ takes integer values from zero to (theoretically) infinity, when chattering ends. Note that Eq. (65) consists of two parts. The first part provides the time-intervals between two consecutive impacts when the

sign of rotation is same as the sign of initial rotation ($i_n = i_0$). The second part provides the time-intervals between two consecutive impacts when the sign of rotation is opposite to the sign of initial rotation ($i_n = -i_0$).

***Iterative procedure***

Equations (62) and (64) form an iterative algorithm that through the coefficients $T_{n;1}$ and $T_{n;3}$, respectively, approximate the chattering time via Eq. (65) that brings the block to rest.

*Step 1*: During the first cycle of rotation $n = 0$ (Fig. 2(b)), Eq. (31) provides the lowest order of approximation $T_{0;1}$ of the chattering time when the first impact ($\tau_1$) happens.

*Step 2*: During the second cycle of rotation $n = 1$ and $i_n = -i_0$ (Fig. 2(b)), Eq. (64) provides the lowest order of approximation $T_{1;3}$ of the chattering time when the second impact ($\tau_2$) happens.

*Step 3*: During the third cycle of rotation $n = 2$ and $i_n = i_0$ (Fig. 2(b)), solution of the cubic equation of Eq. (62) provides the lowest order of approximation $T_{2;1}$ of the chattering time when the third impact ($\tau_3$) happens.

*Next steps*: Steps 2, 3 form an iterative algorithm that are applied consecutively till the cubic equation of Eq. (62) returns a negative solution, which indicates the end of the chattering motion.

## 4 Semi-analytical approximation of the chattering time

This section presents a semi-analytical approach to approximate the chattering time of a rocking block. The aim of this section is, thus, twofold: (i) it verifies the accuracy of the asymptotic scheme proposed in Section 3, and (ii) serves as an alternative method of approximation of the chattering time.

Consider the rocking block of Fig. 1 subjected to a low amplitude (i.e. weak) ground motion (Fig. 2). After a sufficiently large, yet arbitrary, number of impacts $n$, and just before the accumulation point emerges, the time-interval between consecutive impacts becomes orders of magnitude smaller than the period of the ground excitation. Consequently, there exists an $n^{th}$ impact (Fig. 2(c)) after which the ground acceleration appears as a nonzero constant value $\delta$. Under these conditions, the equation of motion of Eq. (4) can be written as:

$$\phi_n^{''}(\tau) - \phi_n(\tau) + sgn(\phi_n) = -\delta, \qquad \tau \le \tau_{ex} \quad (66)$$

where $\tau_{ex}$ is the dimensionless time-instant the ground excitation ends. Without loss of generality, assuming at the time-instant of the $n^{th}$ impact $\tau = \tau_n$ that $i_n = -i_0 > 0$ (Fig. 2(c)), the initial conditions are $\phi_n(\tau_n) = 0$ and $\phi_n^{'}(\tau_n) = \phi_n^{'+} > 0$.

At $\tau = \tau_{n+1}$ (Fig. 2(c)), impact happens, thus solution of Eq. (66) ($\phi_n(\tau_{n+1}) = 0$) yields the time-interval $\Delta\tau_n = \tau_{n+1} - \tau_n$ between two consecutive impacts at $\tau_n$ and $\tau_{n+1}$:

$$\Delta\tau_n = \frac{2}{i_n + \delta}\phi_n^{'+} \quad (67)$$

where $\phi_n^{'+}$ is the post-impact angular velocity of the block at the $n^{th}$ impact, and $i_n$ represents the sign of rocking rotation which is equal to $i_n = \pm 1$. Solution of Eq. (66) also gives the pre-impact angular velocity at $\tau = \tau_{n+1}$ (Fig. 2(c)):

$$\phi_{n+1}^{'-} = -\phi_n^{'+} \quad (68)$$

where, because $\phi_n^{'+} > 0$ it follows $\phi_{n+1}^{'-} < 0$. Equation (68) implies that the pre-impact angular velocity at $\tau = \tau_{n+1}$ is equal (in magnitude) with the post-impact angular velocity at $\tau = \tau_n$. Recall that during forced-rocking, this is not generally true (see e.g. Eq. (58)). However, Eq. (68) represents solely the first order approximation of the angular velocity.

For any subsequent impact $j > n$, Eq. (67) allows for a generalization of the time-interval between two consecutive impacts:

$$\Delta\tau_j = \frac{2}{i_j + \delta}\phi_j^{'+} \quad (69)$$

with:

$$\begin{aligned} &i_{n+1} = (-1)\, i_n = -i_n \\ &i_{n+2} = (-1)^2 i_n = i_n \\ &i_{n+3} = (-1)^3 i_n = -i_n \\ &... \\ &i_j = (-1)^{j-n} i_n \end{aligned} \quad (70)$$

and based on Eq. (68):

$$\begin{aligned} &\phi_{n+1}^{'+} = \eta\phi_{n+1}^{'-} = (-1)\eta\phi_n^{'+} < 0 \\ &\phi_{n+2}^{'+} = \eta\phi_{n+2}^{'-} = (-1)\eta\phi_{n+1}^{'+} = (-1)^2\eta^2\phi_n^{'+} > 0 \\ &\phi_{n+3}^{'+} = \eta\phi_{n+3}^{'-} = (-1)\eta\phi_{n+2}^{'+} = (-1)^3\eta^3\phi_n^{'+} < 0 \\ &... \\ &\phi_j^{'+} = (-1)^{j-n}\eta^{j-n}\phi_n^{'+} \end{aligned} \quad (71)$$

where $\eta$ is the coefficient of restitution. Therefore, when the $(n+3)^{th}$ impact occurs (Fig. 2(c)), Eq. (69) yields:

$$\begin{aligned} \Delta\tau_{n+2} &= \tau_{n+3} - \tau_{n+2} \\ &= \frac{2}{i_{n+2} + \delta}\phi_{n+2}^{'+} = \eta^2 \frac{2}{i_n + \delta}\phi_n^{'+} = \eta^2 \Delta\tau_n \end{aligned} \quad (72)$$

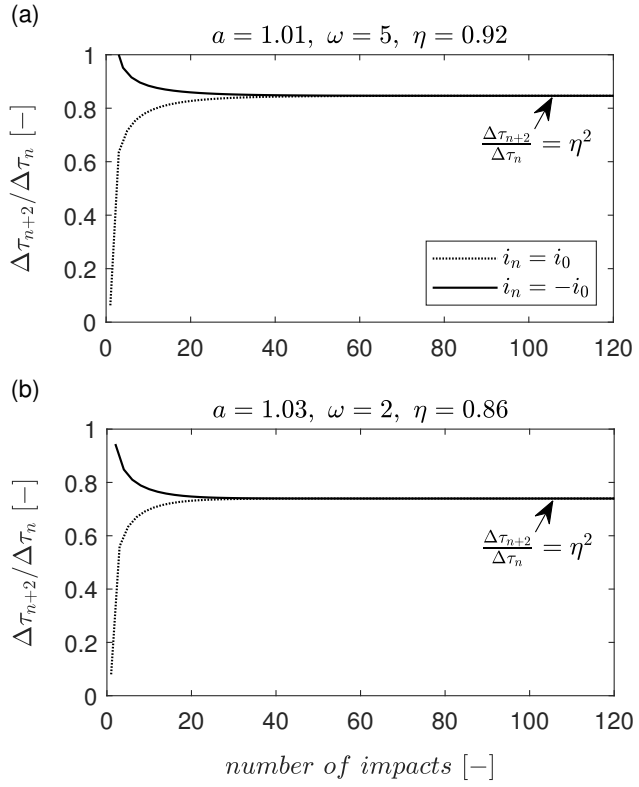


**Fig. 3** Ratio of time-intervals of every two consecutive impacts of the rocking block ($p = 1\ s^{-1}$ and $\alpha = 0.2\ rad$) of Fig. 1 when subjected to sinusoidal ground excitations of amplitude and frequency (a) $a = 1.01$, $\omega = 5$, (b) $a = 1.03$, $\omega = 2$, respectively, and total duration of $T$ (where $T = 2\pi/\omega$ is the period of the ground excitation) for (a) $\eta = 0.92$ and (b) $\eta = 0.86$, respectively.

Interestingly, Eq. (72) reveals that during the chattering oscillations and after a sufficiently large, yet arbitrary, number of impacts, the ratio of the time-intervals of every two consecutive impacts becomes constant and equal to:

$$\frac{\Delta\tau_{n+2}}{\Delta\tau_n} = \eta^2 \tag{73}$$

Figure 3 plots the ratio of the time-intervals of every two consecutive impacts of the rocking block of Fig. 1 when subjected to sinusoidal ground excitations of different amplitude and frequency. Figure 3 shows that even though the ratio $\Delta\tau_{n+2}/\Delta\tau_n$ initially varies, after a sufficient large number of impacts, it becomes constant. Importantly, Fig. 3 verifies numerically Eq. (73) for different values of the coefficient of restitution $\eta$.

From an analytical perspective, Eq. (73) allows for a generalization of the relationship between time-intervals of every two consecutive impacts.

$$\begin{aligned}
&\Delta\tau_{n+2} = \eta^2\Delta\tau_n\\
&\Delta\tau_{n+3} = \eta^2\Delta\tau_{n+1}\\
&\Delta\tau_{n+4} = \eta^2\Delta\tau_{n+2} = \eta^4\Delta\tau_n\\
&\Delta\tau_{n+5} = \eta^2\Delta\tau_{n+3} = \eta^4\Delta\tau_{n+1}\\
&\dots\\
&\Delta\tau_j = \eta^{j-n}\Delta\tau_n\\
&\Delta\tau_{j+1} = \eta^{j-n}\Delta\tau_{n+1}
\end{aligned} \tag{74}$$

Therefore, the chattering time can be approximated as a summation of (i) the first sufficiently large, yet arbitrary, $n$ number of impacts for which the ratio of the time-intervals of every two consecutive impacts varies (see e.g. $n < 60$ in Fig. 3) and (ii) the remaining impacts, till chattering is completed, for which the ratio of the time-intervals of every two consecutive impacts becomes constant.

$$\begin{aligned}
\tau_{ch} = \sum_{i=0}^{\infty}\Delta\tau_i &= \sum_{i=0}^{n-1}\Delta\tau_i + \sum_{i=n}^{\infty}\Delta\tau_i\\
&\cong \sum_{i=0}^{n-1}\Delta\tau_i + \frac{\Delta\tau_n + \Delta\tau_{n+1}}{1-\eta^2}
\end{aligned} \tag{75}$$

which leaves solely the $\sum_{i=0}^{n-1}\Delta\tau_i$, $\Delta\tau_n$ and $\Delta\tau_{n+1}$ time-intervals of consecutive impacts to be numerically determined, thus, the approach is semi-analytical.

## 5 Complete chattering behaviour

For practical applications, it is important to determine under which conditions a rocking block sustains *complete chattering* and comes to rest (while the ground excitation is still active). Therefore, with reference to sinusoidal ground excitations strong enough to trigger rocking motion, but weak enough to not cause overturning, this section further examines the influence complete chattering might have on rocking response through numerical simulations.

### 5.1 Conditions for complete chattering

Consider the rocking block of Fig. 1 subjected to the harmonic sinusoidal ground excitation of Fig. 4. At the time-instant the ground acceleration exceeds the minimum threshold of Eq. (1), rocking initiates (denoted as "1st initiation"). Till the next time-instant the ground acceleration exceeds the minimum threshold (denoted as "2nd" initiation), the block exhibits chattering behaviour due to the weak ground excitation and it might

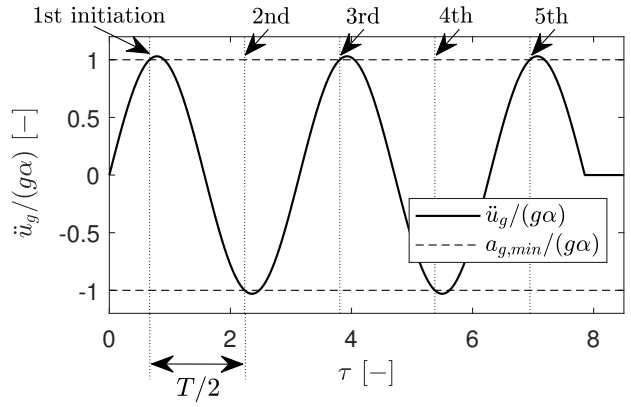


**Fig. 4** Harmonic sinusoidal ground excitation of amplitude $a = 1.03$, frequency $\omega = 2$, and total duration of $2.5T$ (where $T = 2\pi/\omega$ is the period of the ground excitation).

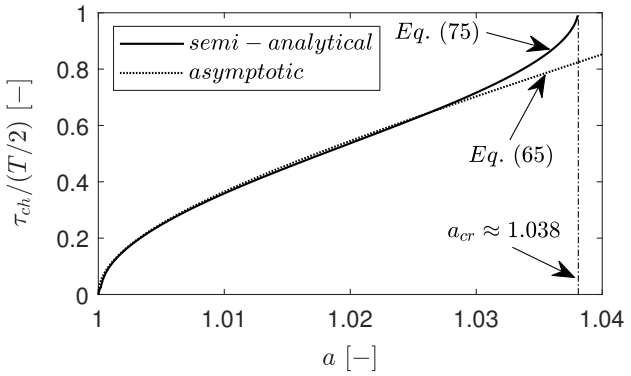


**Fig. 5** Semi-analytical (Eq. (75)) and asymptotic (Eq. (65)) approximation of the chattering time $\tau_{ch}$ over half the period of the ground excitation $T/2$, where $T = 2\pi/\omega$, with respect to the ground acceleration amplitude $a$ for $\eta = 0.92$.

terminate its motion (or not). In case it terminates its motion, it undergoes complete chattering with its rotation and angular velocity becoming zero even though the ground acceleration remains nonzero. An important realization is that complete chattering can potentially occur only within a maximum time-frame of half the period of the sinusoidal ground excitation, i.e. $\tau_{ch} < T/2$, where $\tau_{ch}$ is the (dimensionless) approximated chattering time and $T = 2\pi/\omega$ is the dimensionless period of the ground excitation. $\tau_{ch} = T/2$ is the maximum potential chattering duration, as after $T/2$ the excitation will again become strong enough to restart rocking even from rest conditions.

Under a sinusoidal ground excitation (Fig. 4), the chattering time $\tau_{ch}$ depends on the dimensionless acceleration amplitude $a$ and frequency $\omega$ of the ground excitation (Eq. (5)), and the coefficient of restitution $\eta$ (Eq. (13)). Hence, the ratio of the chattering time over half the period of the ground excitation ($\tau_{ch}/(T/2)$), where $T = 2\pi/\omega$, depends solely on the acceleration amplitude of the excitation $a$ and the coefficient of restitution $\eta$. Figure 5 plots the ratio $\tau_{ch}/(T/2)$ with respect to $a$ for $\eta = 0.92$ when the chattering time is approximated through both the proposed asymptotic scheme of Section 3 (Eq. (65)) and the semi-analytical approach of Section 4 (Eq. (75)). Specifically, Fig. 5 reveals the remarkable agreement between the two methodologies and, importantly, verifies the accuracy of the asymptotic approximation. As expected, $\tau_{ch}/(T/2)$ increases with the amplitude of the excitation. Hence, when $\tau_{ch} = T/2$ the value of ground acceleration amplitude is critical, namely $a_{cr}$ in Fig. 5, because the chattering time becomes equal to half the period of the ground excitation, which is its maximum possible value. For higher values of ground acceleration amplitude ($a > a_{cr}$), complete chattering becomes incomplete and the block does not stop rocking. Observe from Fig. 5 that the chattering time presents two asymptotes; one when rocking initiates (i.e. at $a = 1$), and another one when the chattering behaviour transforms from complete to incomplete (i.e. at $a = a_{cr}$). Interestingly, the asymptotic scheme of Section 3 approximates the chattering time almost perfectly both at the asymptote at $a = 1$ and throughout the ground acceleration range, while it fails at the asymptote at $a = a_{cr}$. However, overall, it can be considered that the asymptotic approximation of the chattering time proposed in Section 3 and manifested through Eq. (65) is adequately accurate.

Figure 6 plots the dimensionless critical acceleration $a_{cr}$ with respect to the frequency of the ground excitation $\omega$ and the coefficient of restitution $\eta$ together with a fitted polynomial function (Eq. (76)):

$$a_{cr} = \frac{a_{g,cr}}{g\alpha} = 1.079 - 0.1885\eta + 0.1405\omega + 0.6442\eta^2 - 0.1903\eta\omega - 0.02818\omega^2 - 0.7372\eta^3 + 0.06413\eta^2\omega + 0.03236\eta\omega^2 + 0.00176\omega^3 + 0.2146\eta^4 - 0.0187\eta^3\omega - 0.003045\eta^2\omega^2 - 0.00185\eta\omega^3 \quad (76)$$

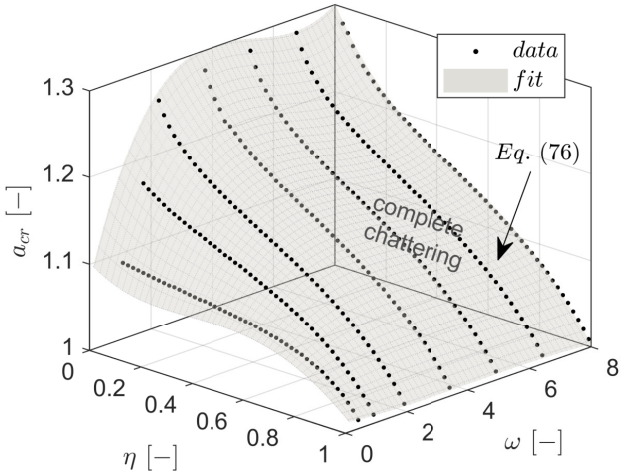


**Fig. 6** Critical ground acceleration amplitude $a_{cr}$, below which complete chattering occurs, with respect to the frequency of the ground excitation $\omega$ and the coefficient of restitution $\eta$.

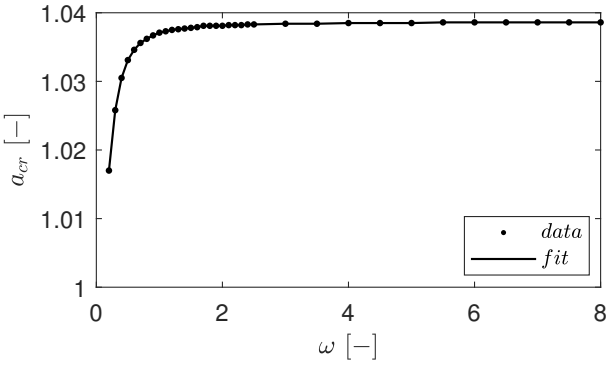


**Fig. 7** Critical ground acceleration amplitude $a_{cr}$ with respect to the frequency of the ground excitation $\omega$ for $\eta = 0.92$.

In particular, Fig. 6 shows that as $\eta$ decreases, more energy is dissipated at each impact, thus, $a_{cr}$ increases regardless of the value of $\omega$. Importantly, Fig. 6 illustrates that as $\eta$ increases, the influence of $\omega$ on the critical acceleration $a_{cr}$ decreases. Thus, for values of $\eta$ within the range of practical interest in rocking dynamics (i.e. $\eta > 0.75$ [24]), $a_{cr}$ can be considered independent of $\omega$.

Figure 7 illustrates such a case, where the critical acceleration $a_{cr}$ is plotted with respect to the frequency of the ground excitation $\omega$ for $\eta = 0.92$. Indeed, Fig. 7 verifies the marginal influence of $\omega$ on $a_{cr}$ as from $\omega = 0.5$ to $\omega = 8$, $a_{cr}$ differs only by 0.5%. Hence, for such cases, a simplified version of Eq. (76), where $a_{cr}$ depends solely on the coefficient of restitution $\eta$, reads:

$$a_{cr} = \frac{a_{g,cr}}{g\alpha} = -0.3941\eta^3 + 0.5763\eta^2 - 0.45\eta + 1.271 \quad (77)$$

Overall, Figs 6, 7 unveil that the critical ground acceleration $a_{cr}$ depends predominately on the coefficient of restitution $\eta$—at least for values of $\eta$ of practical interest. In addition, the value of $a_{cr}$ (Eq. (76) or Eq. (77)) implies that a sinusoidal ground excitation with an acceleration amplitude capable of triggering rocking motion ($a \geq 1$) without overturning, but lower than the critical value ($a < a_{cr}$) leads to complete chattering behaviour. Thus, for $1 < a < a_{cr}$, the block initiates rocking, but approximately after time $\tau_{ch}$, it eventually returns to rest position, without ground motion being zero. If at a subsequent time-instant the ground acceleration exceeds again the minimum threshold for rocking initiation ($a \geq 1$), the block re-initiates its rocking motion.

### 5.2 Complete chattering during the dynamic response of a rocking block

This section investigates the effect of complete chattering on the response-history (response-trajectory) of a rocking block. To this end, it performs numerical simulations by means of two time-integration schemes.

The first scheme is a conventional event-based approach which utilises an angular velocity threshold (denoted as "VelTol") to artificially terminate the chattering oscillations (similar to [9, 10, 27]). According to this approach, if during the integration process the post-impact angular velocity $\phi_n^{'}(\tau_n)$ drops below the assumed threshold, i.e. $|\phi_n^{'}(\tau_n)| \leq VelTol$, the block terminates its rocking motion and returns to rest position with its rotation and angular velocity being zero. This is one of the simplest and most commonly used methods to avoid instability issues caused by the presence of accumulation points, nevertheless, the specific value of the velocity threshold is arbitrary.

The second scheme is an ad hoc (also event-based) approach, which incorporates the proposed asymptotic approximation of Section 3. Specifically, instead of relying on a velocity threshold, it terminates rocking motion if during the numerical integration process the time-instant $\tau_n$ of the $n^{th}$ impact exceeds the approximated chattering time, i.e. $\tau_n \geq \tau_{ch}$. Prerequisite conditions are that the ground excitation is sinusoidal and that its amplitude is lower than the critical ground acceleration amplitude $1 < a < a_{cr}$ (Eq. (76) or Eq. (77)), so complete chattering is expected. The ad hoc scheme re-calculates the chattering time via Eq. (65) if at a subsequent time-instant the ground acceleration exceeds

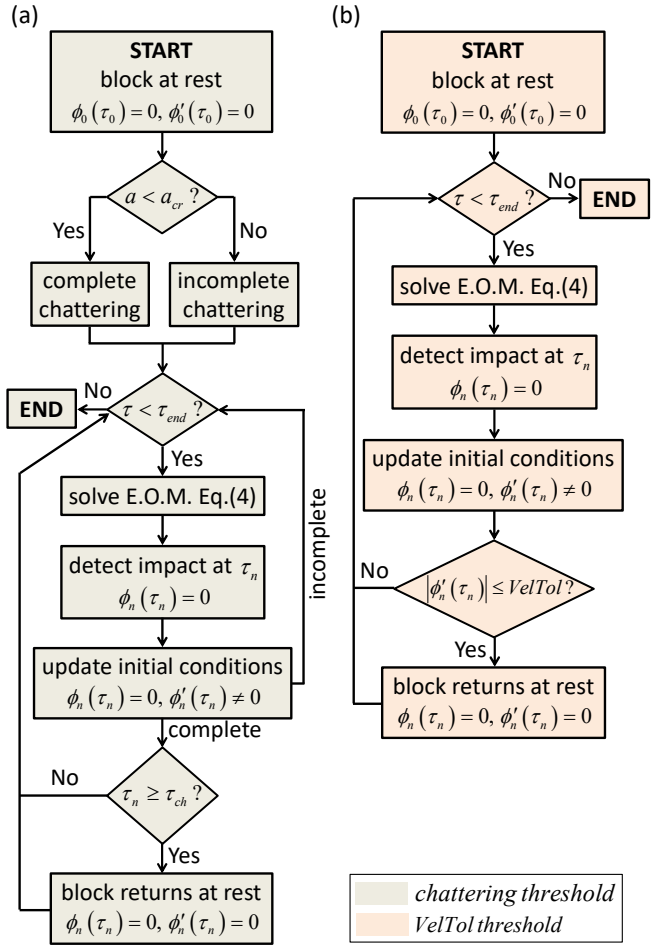


**Fig. 8** Flowchart of the examined event-based time-integration schemes of pure rocking response (i.e. no sliding and bouncing effects) of a block without overturning (a) incorporating the asymptotic scheme of the approximated chattering time of Section 3 and (b) utilizing an angular velocity threshold. Note: $\tau_{end}$ denotes the total duration of analysis.

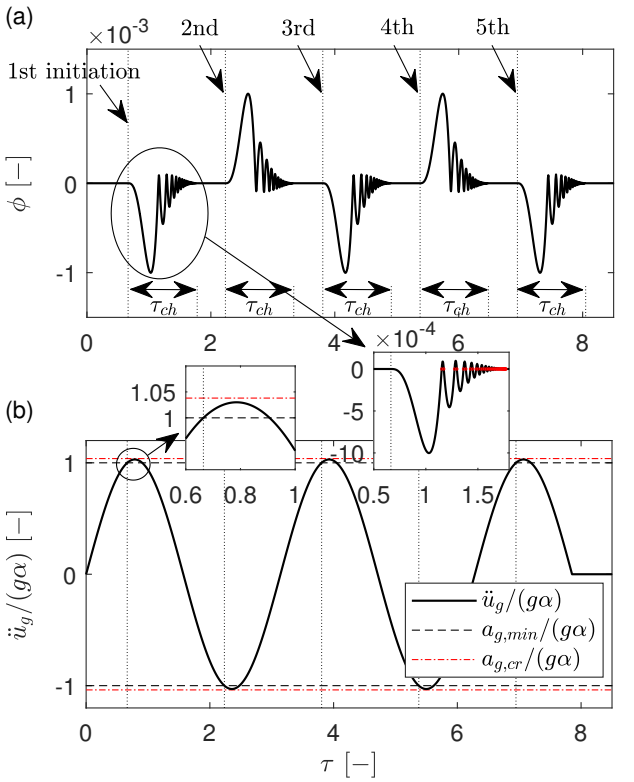


**Fig. 9** (a) Response of the rocking block ($p = 1\ s^{-1}$ and $\alpha = 0.2\ rad$) of Fig. 1 when subjected to (b) a harmonic sinusoidal ground excitation of amplitude $a = 1.03$, frequency $\omega = 2$, and total duration of $2.5T$ (where $T = 2\pi/\omega$ is the period of the ground excitation) for $\eta = 0.92$.

again the minimum threshold for rocking initiation ($a \geq 1$). Figure 8 illustrates the flowchart of both numerical schemes. Note that the aim of this section is not to compare time-integration schemes, but to solely investigate the implications of complete chattering on the response-history (response-trajectory) of the rocking block.

Figure 9 plots the response of the rocking block when subjected to a weak sinusoidal ground excitation of amplitude $a = 1.03$ and frequency $\omega = 2$ adopting the ad hoc simulation scheme of Fig. 8(a). For $\eta = 0.92$, the critical ground acceleration amplitude according to Eq. (76) (or Eq. (77)) is $a_{cr} \approx 1.038$ (Fig. 5). Thus, under a lower ground acceleration amplitude (i.e. $a < a_{cr}$), the rocking block is expected to come to rest following its chattering oscillations. Figure 9 shows that, indeed, after rocking commences (denoted as "1st initiation"), the ground acceleration remains low, thus, the block sustains multiple impacts and returns to its initial rest position after completing its chattering oscillations, namely approximately after $\tau_{ch}$ (Eq. (65)). Later, it re-initiates its motion (denoted as "2nd" initiation) when the next lobe of (opposite sign) ground acceleration triggers rocking motion ($a \geq 1$). Observe from the insert of Fig. 9(a) that the number of impacts the block exhibits before coming to rest, while theoretically infinite, numerically is finite (and it is also experimentally) [8]. Regardless, what is most important is that the block terminates its rocking motion even though it is still subjected to nonzero ground excitation. This fact has not received the attention that deserves in earthquake engineering.

Figures 10, 11 plot the response of the rocking block when subjected to harmonic sinusoidal ground excitations of different (low) amplitude, i.e. $a = 1.03$, $a = 1.05$, respectively, and frequency $\omega = 2$ adopting both simulation approaches, namely "chattering threshold" and "VelTol threshold" (Fig. 8). The main difference between Fig. 10 and Fig. 11 lies in that the ground acceleration amplitude in Fig. 10 is lower than the critical acceleration amplitude $a < a_{cr}$ (Eq. (76) or Eq. (77)),

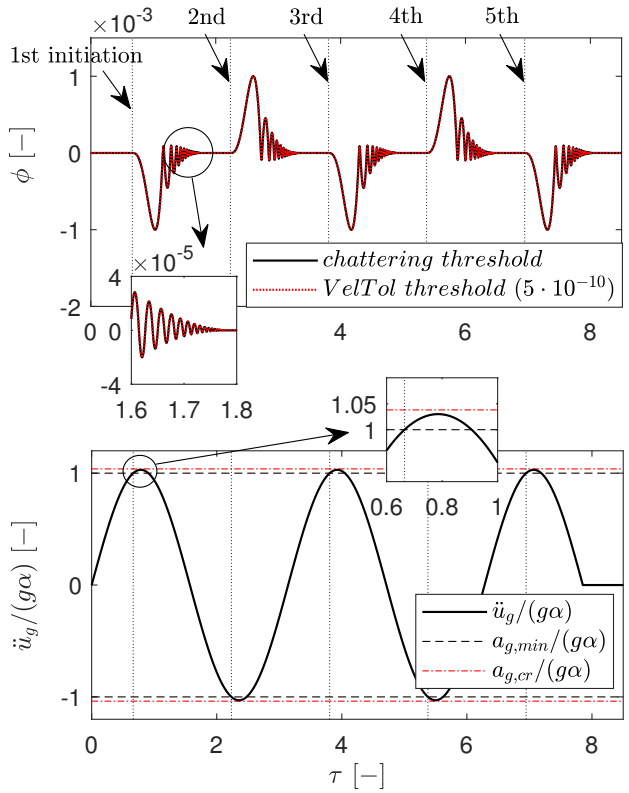


**Fig. 10** Response of the rocking block ($p = 1\ s^{-1}$ and $\alpha = 0.2\ rad$) of Fig. 1 when subjected to a harmonic sinusoidal ground excitation of amplitude $a = 1.03$, frequency $\omega = 2$, and total duration of $2.5T$ (where $T = 2\pi/\omega$ is the period of the ground excitation) for $\eta = 0.92$. Note: $VelTol/(p\alpha) = 5 \cdot 10^{-10}$ for the "VelTol threshold" simulation.

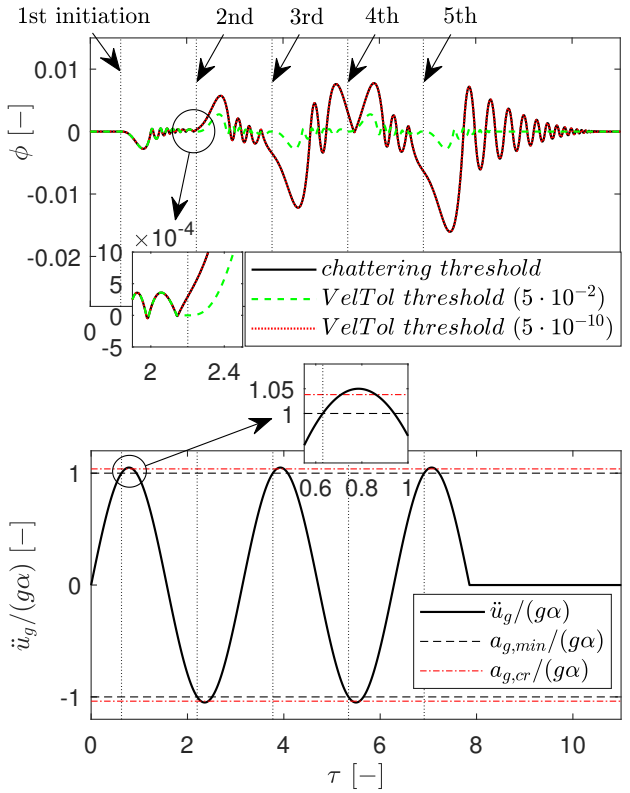


**Fig. 11** Response of the rocking block ($p = 1\ s^{-1}$ and $\alpha = 0.2\ rad$) of Fig. 1 when subjected to a harmonic sinusoidal ground excitation of amplitude $a = 1.05$, frequency $\omega = 2$, and total duration of $2.5T$ (where $T = 2\pi/\omega$ is the period of the ground excitation) for $\eta = 0.92$. Note: $VelTol/(p\alpha) = 5 \cdot 10^{-2}$ and $VelTol/(p\alpha) = 5 \cdot 10^{-10}$ for the "VelTol threshold" simulations.

thus, complete chattering is expected. On the contrary, the amplitude of the ground acceleration in Fig. 11 is higher than the critical value $a > a_{cr}$, hence, incomplete chattering is expected. Recall that for $\eta = 0.92$, it follows $a_{cr} \approx 1.038$ (Eq. (76) or Eq. (77)) (Fig. 5). In addition, Figs 10, 11 reveal the sensitivity of the rocking response on the value of the velocity threshold. As a first approach, Fig. 10 shows that both simulation approaches predict complete chattering (since $a < a_{cr}$) and terminate properly the motion of the block. In particular, after rocking commences (denoted as "1st initiation"), due to the weak, yet nonzero, ground excitation, the block sustains complete chattering and returns to its initial rest position after multiple impacts (see insert of Fig. 10). The block re-initiates its motion (denoted as "2nd" initiation) with zero initial conditions (i.e. rotation and angular velocity) when the next lobe of (opposite sign) ground acceleration is capable of triggering rocking motion ($a \geq 1$). In contrast, in Fig. 11 incomplete chattering is expected since $a > a_{cr}$. In particular, if during the chattering oscillations of the rocking block, its (post-impact) angular velocity drops below the assumed threshold, the block comes to rest even though it should not have. Subsequently, it enters its next cycle of rotation with zero initial conditions which results in a completely different response-history (response-trajectory). The insert of Fig. 11 clearly illustrates the details of motion termination and subsequently the conditions of rocking re-initiation, when an "improper" value of velocity threshold is adopted. In summary, Figs 10, 11 reveal that the ad hoc "chattering threshold" simulation approach is robust and depends solely on the ground acceleration amplitude criterion of Eq. (76) (or Eq. (77)) that dictates whether chattering is complete or incomplete. The ad hoc simulation approach, though, is applicable only to sinusoidal ground excitations.

Overall, Figs 10, 11, unveil that the chattering phenomenon should not be overlooked when the amplitude of the sinusoidal ground acceleration falls within $1 < a < a_{cr}$. Moreover, in (conventional) event-based simulations, the value of the velocity threshold should be carefully selected. For more complicated waveforms,

i.e. consisted of more lobes of different amplitude or realistic (historic) earthquake records, the influence of complete chattering could be even more complicated and merits further investigation. Currently, no criteria for the appearance of complete chattering, or estimations of its duration, exist for more complicated ground excitation waveforms.

## 6 Conclusions

The present paper focuses on the *chattering* behaviour of a freestanding rocking block when subjected to a sinusoidal ground excitation of low amplitude. Chattering is a highly nonlinear phenomenon that can have substantial influence on the dynamic response. Specifically, complete chattering refers to the phenomenon during which the block undergoes a theoretically infinite sequence of decaying impacts, in finite time, which eventually bring the block to rest even under nonzero ground excitation. This study investigates the conditions under which complete chattering brings the block to rest, and the corresponding (chattering) time needed for this to happen. To this end, this study adopts perturbation theory and conducts asymptotic analysis.

Specifically, this paper provides an asymptotic scheme that efficiently approximates chattering time, contributing with a state-of-the-art mathematical formulation of the chattering phenomenon for the rocking problem. Note that the proposed asymptotic scheme is also verified through an independent semi-analytical approximation. In addition, this work proposes a ground acceleration amplitude threshold (for sinusoidal ground excitations) below which complete chattering occurs. Importantly, numerical simulations reveal the influence complete chattering might have on the dynamic response of a rocking block. These results suggest that chattering should not be overlooked when the ground acceleration amplitude is barely capable of triggering rocking motion without overturning or when random ground motions replicating earthquakes are considered.

**Acknowledgements** The authors would like to thank Professor Stefano Lenci from Polytechnic University of Marche, Italy, and the anonymous reviewers, for providing comments and suggestions to further improve the current work.

**Funding** This study has been funded by the STAND4-HERITAGE project (new STANDards FOR seismic assessment of built cultural HERITAGE) that has received funding from the European Research Council (ERC) under the European Union's Horizon 2020 research and innovation program (Grant No. 833123) as an Advanced Grant. Its support is gratefully acknowledged. The opinions and conclusions presented in this paper are those of the authors and do not necessarily reflect the views of the sponsoring organization.

**Data availability** Data generated during this study are available from the corresponding author on reasonable request.

**Conflict of interest** The authors declare that they have no conflict of interest.

## References

1. Acary, V.: Projected event-capturing time-stepping schemes for nonsmooth mechanical systems with unilateral contact and coulomb's friction. Computer Methods in Applied Mechanics and Engineering **256**, 224–250 (2013)
2. Agalianos, A., Psychari, A., Vassiliou, M.F., Stojadinovic, B., Anastasopoulos, I.: Comparative assessment of two rocking isolation techniques for a motorway overpass bridge. Frontiers in Built Environment **3**, 47 (2017)
3. Ames, A.D., Zheng, H., Gregg, R.D., Sastry, S.: Is there life after zeno? taking executions past the breaking (zeno) point. In: 2006 American control conference, pp. 6–pp. IEEE (2006)
4. Aslam, M., Scalise, D.T., Godden, W.G.: Earthquake rocking response of rigid bodies. Journal of the Structural Division **106**(2), 377–392 (1980)
5. Baranyai, T., Várkonyi, P.L.: Zeno chattering of rigid bodies with multiple point contacts. Nonlinear Dynamics **92**(4), 1857–1879 (2018)
6. Brogliato, B.: Nonsmooth mechanics: models, dynamics and control. Springer (1999)
7. Brogliato, B., Zhang, H., Liu, C.: Analysis of a generalized kinematic impact law for multibody-multicontact systems, with application to the planar rocking block and chains of balls. Multibody System Dynamics **27**(3), 351–382 (2012)
8. Budd, C., Dux, F.: Chattering and related behaviour in impact oscillators. Philosophical Transactions of the Royal Society of London. Series A: Physical and Engineering Sciences **347**(1683), 365–389 (1994)
9. Chatterjee, A., Rodriguez, A., Bowling, A.: Analytic solution for planar indeterminate impact problems using an energy constraint. Multibody System Dynamics **42**(3), 347–379 (2018)
10. Cosimo, A., Cavalieri, F.J., Cardona, A., Brüls, O.: On the adaptation of local impact laws for multiple impact problems. Nonlinear Dynamics **102**(4), 1997–2016 (2020)

11. Cusumano, J., Bai, B.Y.: Period-infinity periodic motions, chaos, and spatial coherence in a 10 degree of freedom impact oscillator. Chaos, Solitons & Fractals **3**(5), 515–535 (1993)
12. DeJong, M.J., Dimitrakopoulos, E.G.: Dynamically equivalent rocking structures. Earthquake Engineering & Structural Dynamics **43**(10), 1543–1563 (2014)
13. Demeio, L., Lenci, S.: Asymptotic analysis of chattering oscillations for an impacting inverted pendulum. The Quarterly Journal of Mechanics & Applied Mathematics **59**(3), 419–434 (2006)
14. Demeio, L., Lenci, S.: Dynamic analysis of a ball bouncing on a flexible beam. Journal of Sound and Vibration **441**, 152–164 (2019)
15. Dimitrakopoulos, E.G., DeJong, M.J.: Overturning of retrofitted rocking structures under pulse-type excitations. Journal of Engineering Mechanics **138**(8), 963–972 (2012)
16. Dimitrakopoulos, E.G., DeJong, M.J.: Revisiting the rocking block: closed-form solutions and similarity laws. Proceedings of the Royal Society A: Mathematical, Physical and Engineering Science **468**(2144), 2294–2318 (2012)
17. Dimitrakopoulos, E.G., Fung, E.D.W.: Closed-form rocking overturning conditions for a family of pulse ground motions. Proceedings of the Royal Society A: Mathematical, Physical and Engineering Science **472**(2196), 20160662 (2016)
18. Dimitrakopoulos, E.G., Giouvanidis, A.I.: Seismic response analysis of the planar rocking frame. Journal of Engineering Mechanics **141**(7), 04015003 (2015)
19. Dimitrakopoulos, E.G., Paraskeva, T.S.: Dimensionless fragility curves for rocking response to near-fault excitations. Earthquake Engineering & Structural Dynamics **44**(12), 2015–2033 (2015)
20. ElGawady, M.A., Sha'lan, A.: Seismic behavior of self-centering precast segmental bridge bents. Journal of Bridge Engineering **16**(3), 328–339 (2010)
21. Fardis, M.N.: Uplift of deck or footings in bridges with distributed mass subjected to transverse earthquake. Earthquake Engineering & Structural Dynamics **44**(15), 2755–2773 (2015)
22. Fragiadakis, M., Diamantopoulos, S.: Fragility and risk assessment of freestanding building contents. Earthquake Engineering & Structural Dynamics **49**(10), 1028–1048 (2020)
23. Funari, M.F., Mehrotra, A., Lourenço, P.B.: A tool for the rapid seismic assessment of historic masonry structures based on limit analysis optimisation and rocking dynamics. Applied Sciences **11**(3), 942 (2021)
24. Galvez, F., Sorrentino, L., Dizhur, D., Ingham, J.M.: Seismic rocking simulation of unreinforced masonry parapets and façades using the discrete element method. Earthquake Engineering & Structural Dynamics (2022)
25. Giouvanidis, A.I., Dimitrakopoulos, E.G.: Nonsmooth dynamic analysis of sticking impacts in rocking structures. Bulletin of Earthquake Engineering **15**(5), 2273–2304 (2017)
26. Giouvanidis, A.I., Dimitrakopoulos, E.G.: Seismic performance of rocking frames with flag-shaped hysteretic behavior. Journal of Engineering Mechanics **143**(5), 04017008 (2017)
27. Giouvanidis, A.I., Dimitrakopoulos, E.G.: Rocking amplification and strong-motion duration. Earthquake Engineering & Structural Dynamics **47**(10), 2094–2116 (2018)
28. Giouvanidis, A.I., Dong, Y.: Seismic loss and resilience assessment of single-column rocking bridges. Bulletin of earthquake engineering **18**(9), 4481–4513 (2020)
29. Goebel, R., Teel, A.R.: Lyapunov characterization of zeno behavior in hybrid systems. In: 2008 47th IEEE Conference on Decision and Control, pp. 2752–2757. IEEE (2008)
30. Goyal, S., Papadopoulos, J., Sullivan, P.: The dynamics of clattering i: Equation of motion and examples. Journal of Dynamic Systems, Measurement, and Control **120**(1), 83–93 (1998)
31. Goyal, S., Papadopoulos, J., Sullivan, P.: The dynamics of clattering ii: Global results and shock protection. Journal of Dynamic Systems, Measurement, and Control **120**(1), 94–102 (1998)
32. Hatchell, P.J.: Investigating $t_\infty$ for bouncing balls. American Journal of Physics **89**(2), 147–156 (2021)
33. Hogan, S.: On the dynamics of rigid-block motion under harmonic forcing. Proceedings of the Royal Society of London A: Mathematical, Physical and Engineering Sciences **425**(1869), 441–476 (1989)
34. Holmes, M.H.: Introduction to perturbation methods, vol. 20. Springer Science & Business Media (2012)
35. Housner, G.W.: The behavior of inverted pendulum structures during earthquakes. Bulletin of the Seismological Society of America **53**(2), 403–417 (1963)
36. Jean, M.: The non-smooth contact dynamics method. Computer Methods in Applied Mechanics and Engineering **177**(3-4), 235–257 (1999)
37. Jeong, M., Suzuki, K., Yim, S.C.: Chaotic rocking behavior of freestanding objects with sliding motion. Journal of sound and vibration **262**(5), 1091–1112 (2003)

38. Kalliontzis, D., Sritharan, S., Schultz, A.: Improved coefficient of restitution estimation for free rocking members. Journal of Structural Engineering **142**(12), 06016002 (2016)
39. Kazantzi, A.K., Lachanas, C.G., Vamvatsikos, D.: Seismic response distribution expressions for on-ground rigid rocking blocks under ordinary ground motions. Earthquake Engineering & Structural Dynamics (2021). DOI 10.1002/eqe.3511
40. Konstantinidis, D., Makris, N.: Experimental and analytical studies on the response of 1/4-scale models of freestanding laboratory equipment subjected to strong earthquake shaking. Bulletin of Earthquake Engineering **8**(6), 1457–1477 (2010)
41. Lamperski, A., Ames, A.D.: Lyapunov theory for zeno stability. IEEE Transactions on Automatic Control **58**(1), 100–112 (2012)
42. Le Saux, C., Leine, R.I., Glocker, C.: Dynamics of a rolling disk in the presence of dry friction. Journal of Nonlinear Science **15**(1), 27–61 (2005)
43. Leine, R.I., Heimsch, T.: Global uniform symptotic attractive stability of the non-autonomous bouncing ball system. Physica D: Nonlinear Phenomena **241**(22), 2029–2041 (2012)
44. Lenci, S., Demeio, L., Petrini, M.: Response scenario and nonsmooth features in the nonlinear dynamics of an impacting inverted pendulum. Journal of computational and nonlinear dynamics **1**(1), 56–64 (2006)
45. Lenci, S., Rega, G.: A dynamical systems approach to the overturning of rocking blocks. Chaos, Solitons & Fractals **28**(2), 527–542 (2006)
46. Lin, H., Yim, S.: Nonlinear rocking motions. i: chaos under noisy periodic excitations. Journal of Engineering Mechanics **122**(8), 719–727 (1996)
47. Luck, J.M., Mehta, A.: Bouncing ball with a finite restitution: chattering, locking, and chaos. Physical Review E **48**(5), 3988 (1993)
48. Lyapunov, A.M.: Stability of motion. Academic Press (1966)
49. Makris, N., Vassiliou, M.F.: Planar rocking response and stability analysis of an array of free-standing columns capped with a freely supported rigid beam. Earthquake Engineering & Structural Dynamics **42**(3), 431–449 (2013)
50. Moreau, J.J.: Unilateral contact and dry friction in finite freedom dynamics. In: Nonsmooth Mechanics and Applications, pp. 1–82. Springer (1988)
51. Nordmark, A.B., Piiroinen, P.T.: Simulation and stability analysis of impacting systems with complete chattering. Nonlinear Dynamics **58**(1), 85–106 (2009)
52. Or, Y., Ames, A.D.: Stability and completion of zeno equilibria in lagrangian hybrid systems. IEEE Transactions on Automatic Control **56**(6), 1322–1336 (2010)
53. Or, Y., Teel, A.R.: Zeno stability of the set-valued bouncing ball. IEEE Transactions on Automatic Control **56**(2), 447–452 (2010)
54. Palermo, A., Pampanin, S.: Enhanced seismic performance of hybrid bridge systems: Comparison with traditional monolithic solutions. Journal of Earthquake Engineering **12**(8), 1267–1295 (2008)
55. Reggiani Manzo, N., Vassiliou, M.F.: Displacement-based analysis and design of rocking structures. Earthquake Engineering & Structural Dynamics **48**(14), 1613–1629 (2019)
56. Reggiani Manzo, N., Vassiliou, M.F.: Simplified analysis of bilinear elastic systems exhibiting negative stiffness behavior. Earthquake Engineering & Structural Dynamics **50**(2), 580–600 (2021)
57. Schindler, K., Leine, R.I.: Paradoxical simulation results of chaos-like chattering in the bouncing ball system. Physica D: Nonlinear Phenomena **419**, 132854 (2021)
58. Shaw, S.W., Rand, R.H.: The transition to chaos in a simple mechanical system. International Journal of Non-Linear Mechanics **24**(1), 41–56 (1989)
59. Thomaidis, I.M., Kappos, A.J., Camara, A.: Dynamics and seismic performance of rocking bridges accounting for the abutment-backfill contribution. Earthquake Engineering & Structural Dynamics **49**(12), 1161–1179 (2020)
60. Vassiliou, M.F.: Seismic response of a wobbling 3d frame. Earthquake Engineering & Structural Dynamics **47**(5), 1212–1228 (2017)
61. Vassiliou, M.F., Sieber, M.: Dimensionality reduction of the 3d inverted pendulum cylindrical oscillator and applications on sustainable seismic design of bridges. Earthquake Engineering & Structural Dynamics (2021). DOI 10.1002/eqe.3575
62. Vassiliou, M.F., Truniger, R., Stojadinovic, B.: An analytical model of a deformable cantilever structure rocking on a rigid surface: development and verification. Earthquake Engineering & Structural Dynamics **44**(15), 2775–2794 (2015)
63. Vlachakis, G., Giouvanidis, A.I., Mehrotra, A., Lourenço, P.B.: Numerical block-based simulation of rocking structures using a novel universal viscous damping model. Journal of Engineering Mechanics **147**(11), 04021089 (2021)
64. Voyagaki, E., Psycharis, I.N., Mylonakis, G.: Complex response of a rocking block to a full-cycle pulse. Journal of Engineering Mechanics **140**(6), 04014024 (2013)

65. Wagg, D.J., Bishop, S.: Chatter, sticking and chaotic impacting motion in a two-degree of freedom impact oscillator. International Journal of Bifurcation and Chaos **11**(01), 57–71 (2001)